The Canadian Mineralogist
Vol. 40, pp. 1313-1338 (2002)

MINERALOGICAL AND GEOCHEMICAL STUDY OF THE REGAL RIDGE EMERALD SHOWING, SOUTHEASTERN YUKON

Lee A. GROAT[§]

Department of Earth and Ocean Sciences, University of British Columbia, Vancouver, British Columbia V6T 1Z4, Canada

Daniel D. MARSHALL

Department of Earth Sciences, Simon Fraser University, Burnaby, British Columbia V5A 1S6, Canada

Gaston GIULIANI

IRD and Centre de Recherches Pétrographiques et Géochimiques/CNRS, UPR 2300, 15, rue Notre Dame des Pauvres,
BP 20, F-54501 Vandœuvre-lès-Nancy Cedex, France

Donald C. MURPHY

Yukon Geology Program, Government of the Yukon, Box 2703 (F-3), Whitehorse, Yukon Y1A 2C6, Canada

Stephen J. PIERCEY, John L. JAMBOR and James K. MORTENSEN

Department of Earth and Ocean Sciences, University of British Columbia, Vancouver, British Columbia V6T 1Z4, Canada

T. Scott ERCIT and Robert A. GAULT

Research Division, Canadian Museum of Nature, P.O. Box 3443, Station D, Ottawa, Ontario K1P 6P4, Canada

David P. MATTEY

Geology Department, Royal Holloway University of London, Egham Hill, Egham, Surrey TW20 0EX, U.K.

Dietmar SCHWARZ

Gübelin Gemmological Laboratory, Maihofstrasse 102, CH-6000 Lucerne 9, Switzerland

Henri MALUSKI

Laboratoire de Géochronologie, Université de Montpellier 2, Place Eugène Bataillon, F-34095 Montpellier, France

Michael A. WISE

Smithsonian Institution, Mineral Sciences NHB119, Washington, D.C. 20560-0119, U.S.A.

William WENGZYNOWSKI and Douglas W. EATON

Expatriate Resources Limited and Archer Cathro & Associates (1981) Limited, 1016-510 West Hastings Street, Vancouver,
British Columbia V6B 1L8, Canada

[§] *E-mail address*: lgroat@ubc.ca

ABSTRACT

In September, 1998, one of the authors (WW) discovered a major occurrence of emerald in the Finlayson Lake district of southeastern Yukon. The Regal Ridge showing occurs in complexly deformed metavolcanic rocks in the Yukon–Tanana Terrane, near their contact with a mid-Cretaceous granitic pluton. The emerald crystals occur where quartz veins cut mica-rich layers in a shallowly dipping mica schist of the Upper Devonian Fire Lake mafic metavolcanic unit. At least eight such veins have been found. Most are surrounded by a much more extensive, overlapping mass of fine, dark tourmaline crystals. The tourmaline crystals are locally associated with minor amounts of scheelite, and small amounts of sulfides have been observed to occur within the quartz veins. A zone of sparse, disseminated sulfides apparently coincides with the tourmaline zone, which is surficially marked by ochreous products of oxidation. Green beryl crystals up to 4 cm in length occur in tourmaline zones and, rarely, in the quartz veins. Some of the smaller crystals, and sections of larger crystals, are of gem quality. The Cr content (average 3208 ppm) shows that it is the predominant chromophore. Fluid-inclusion data indicate that the emerald precipitated from a fluid whose maximum salinity was 3 wt.% NaCl equivalent. The oxygen isotopic composition of the emerald is highly variable (12.3 to 14.8‰), but there is little difference in corresponding δD values (–57.3 and –59.8‰, respectively), which suggests the presence of an isotopically homogeneous fluid that underwent isotopic exchange with the host rocks without achieving homogenization. The $\delta^{18}O$ values for coexisting quartz and tourmaline from the quartz veins yield temperatures of formation of approximately 365 and 498°C. Based on fluid-inclusion isochoric data, these temperatures correspond to pressures of 1.0 to 2.5 kbar, and inferred depths of 3 to 7.7 km. The close proximity of the granite suggests that it is the source of the Be, although the Be content is low (12 and 13.2 ppm). The source of the Cr is the schist (520 ppm Cr). An $^{40}Ar/^{39}Ar$ age of 109 Ma for a mica sample from the schist could either reflect a thermal overprint age related to the event that produced the emerald crystals, or cooling following intrusion of the adjacent pluton, or both.

Keywords: emerald deposit, geology, mineralogy, geochemistry, fluid inclusions, stable isotopes, Finlayson Lake, Yukon, Canada.

SOMMAIRE

En septembre 1998, un des auteurs (WW) a découvert un indice important de minéralisation en émeraude dans la région du lac Finlayson, dans le secteur sud-est du Yukon. L'indice de Regal Ridge est situé dans les roches métavolcaniques déformées de façon complexe dans le socle de Yukon–Tanana, près du contact avec un pluton granitique mis en place au crétacé moyen. Les cristaux d'émeraude se sont développés où des veines de quartz recoupent des niveaux micacés de l'unité schisteuse tardi-dévonienne de Fire Lake, mafique et à faible pendage. Au moins huit veines semblables ont été repérées. Dans la plupart des cas, les veines sont entourées d'une masse de petits cristaux enchevêtrés de tourmaline foncée. Leurs sont associés localement de petites quantités de scheelite, et, dans les veines elles-mêmes, des sulfures. Une zone de sulfures épars coïnciderait avec la zone à tourmaline, marquée par des produits d'oxydation ochres. Des cristaux de béryl vert atteignent 4 cm en longueur dans les zones à tourmaline et, dans certains cas, les veines de quartz. Certains des plus petits cristaux, et des portions des plus gros, ont une qualité gemme. La teneur en Cr (moyenne 3208 ppm) en fait le chromophore principal. Les données sur les inclusions fluides indiquent que la phase fluide responsable de la minéralisation avait une salinité maximale équivalente à 3% de NaCl. La composition isotopique de l'oxygène de l'émeraude est très variable (entre 12.3 et 14.8‰), mais sans variation comparable dans les valeurs de δD correspondantes (–57.3 et –59.8‰, respectivement), ce qui suppose une phase fluide isotopiquement homogène qui a amorcé un échange isotopique avec l'encaissant sans toutefois atteindre l'équilibre. Les valeurs de $\delta^{18}O$ du quartz et de la tourmaline des veines de quartz indiquent une température de formation d'environ 365 et 498°C. A la lumière des données isochores des inclusions fluides, ces températures correspondraient à une pression entre 1.0 et 2.5 kbar, et donc une profondeur entre 3 et 7.7 km. La proximité du granite fait penser qu'il était la source du béryllium, quoique sa teneur en Be est assez faible (entre 12 et 13.2 ppm). La source du Cr est le schiste (520 ppm Cr). Un âge $^{40}Ar/^{39}Ar$ d'un échantillon de mica du schiste, 109 Ma, pourrait témoigner de l'âge d'un réchauffement lié à la minéralisation, ou bien un refroidissement suivant la mise en place du granite, ou les deux.

(Traduit par la Rédaction)

Mots-clés: gisement d'émeraude, géologie, minéralogie, géochimie, inclusions fluides, isotopes stables, lac Finlayson, Yukon, Canada.

INTRODUCTION

In September 1998, W. Wengzynowski discovered a showing of green beryl and emerald (green gem-quality beryl) crystals on Expatriate Resources Limited's Goal Net property, in the Finlayson Lake district of southeastern Yukon (61°16.6'N, 130°35.5'W, NTS 105G/7; Fig. 1). In less than two hours, he collected approximately 1 kg of beryl and emerald from float and outcrop on both sides of an E–W-trending ridge. Detailed work on the property began in July 1999; by late August, numerous green beryl- and emerald-bearing float trains and six main sources (4, 6–7, 9, 10, 14, R) had been discovered in a 900 by 400 m area on both sides of the ridge. Washing and hand sorting of approximately 6 m^3 of material from float trains and trenches yielded more than 6 kg of green beryl and emerald crystals. In mid-2001, True North Gems Inc. entered into an

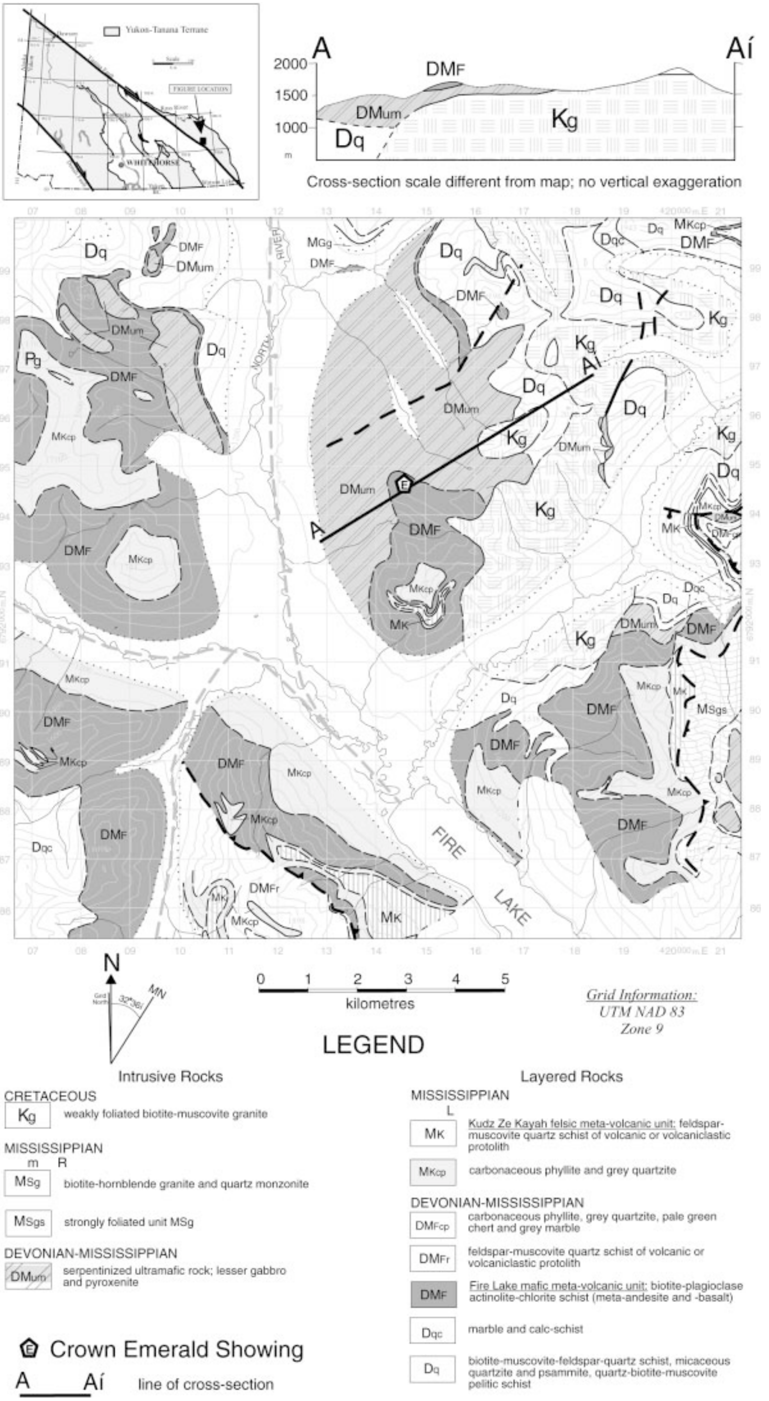

FIG. 1. Map of the southern part of the Yukon Territory showing major geological features and the area shown in Figure 2a.

option agreement with Expatriate Resources Limited to acquire a 50% interest in the property. True North has planned an evaluation program of mechanical trenching and geological and geochemical surveys for the Regal Ridge showing, Canada's first significant emerald discovery.

The objectives of this study were to describe the geology and the mineralogy of the showing and to investigate its origin. The eventual goal is to develop guidelines for exploration, in hopes that additional emerald occurrences will be discovered in the northern Canadian Cordillera.

Geology

The emerald showing occurs in complexly deformed metamorphic rocks of greenschist to lower amphibolite grade in the Yukon–Tanana Terrane, near their contact with a mid-Cretaceous granitic pluton (Figs. 1, 2). Northeast of the Tintina Fault, where the showing occurs, the Yukon–Tanana Terrane is composed of mainly pre-Late Devonian quartz-rich metaclastic rocks and carbonates and Late Devonian and Mississippian metavolcanic and metaplutonic rocks. The metavolcanic rocks host the recently discovered Kudz Ze Kayah, GP4F, Wolverine and Fyre Lake massive sulfide deposits (Murphy 1998a) and are inferred to have formed in continental magmatic arc (Mortensen & Jilson 1985, Mortensen 1992, Murphy 1998a, Murphy & Piercey 2000) and back-arc settings (Piercey *et al.* 2000a, b). These rocks were deformed and imbricated in the Late Paleozoic and again in the Early Cretaceous before the emplacement of a suite of *ca.* 112 Ma peraluminous granitic intrusions (Mortensen 1999, Mortensen & Murphy, unpubl. data).

The emerald crystals occur where quartz veins cut mica-rich layers in a shallowly dipping mica schist of the Upper Devonian Fire Lake mafic metavolcanic unit [unit 2 of Murphy (1997) and Murphy & Piercey (1998), unit DMF of Murphy & Piercey (2000)]. The oldest volcanic unit in the arc – back-arc succession, the Fire Lake unit, is laterally extensive and hosts the Fyre Lake Cu–Co–Au massive sulfide deposit about 6 km southeast of the Regal Ridge showing. The unit is compositionally diverse, including boninite [$SiO_2 > 53\%$, $MgO/(MgO + FeO) > 0.60$], low-Ti tholeiite, normal mid-ocean-ridge basalt (N–MORB), and transitional tholeiite enriched in the light-rare-earth elements (*LREE*) (Piercey *et al.* 1999). In the area of the Regal Ridge showing, the Fire Lake unit comprises metabasalt of boninitic composition (Piercey *et al.* 1999) and overlies a thick, laterally tapering slab of variably serpentinized mafic and ultramafic metaplutonic rocks. Using various geometrical and geological criteria, Murphy (1998a, b) and Murphy & Piercey (2000) interpreted this slab as a comagmatic sill that intruded laterally from feeder dikes localized along a nearby synvolcanic fault.

Structurally, the quartz veins associated with the emerald mineralization are undeformed and discordant with respect to the main foliation affecting the Fire Lake unit near the Regal Ridge showing. This prominent foliation belongs to a set of fabric elements that is part of at least the second phase of deformation of these rocks, and is mid-Cretaceous in age. The foliation is axial planar to tight with respect to isoclinal, south-vergent, outcrop-scale folds that are imposed on an earlier foliation; in the hinges of these folds, the prominent foliation is a crenulation cleavage. Compositional layering and the prominent foliation are deflected by a set of south-vergent shear bands. Mutual cross-cutting relationships between folds and shear bands demonstrate that they formed together. The contact of a nearby Cretaceous intrusion (*ca.* 113 Ma, Mortensen 1999) cross-cuts the prominent foliation, but is itself weakly foliated and cut by shear bands, thereby suggesting that the pluton was intruded during the waning stages of deformation. Further supporting a Cretaceous age for the prominent foliation are several Ar–Ar biotite ages that range from 109 to 113 Ma for the rocks in the area (Murphy & Villeneuve, unpubl. data).

The quartz veins associated with the emerald mineralization range in width from approximately 0.5 to 1.0 m. At least eight such veins have been found on the north side of the ridge. Most are surrounded by a much more extensive, overlapping mass of fine, dark tourmaline crystals. The tourmaline crystals are locally associated with minor amounts of scheelite, and small amounts of sulfides, especially chalcopyrite, have been observed to occur within the quartz veins. A zone of sparse, disseminated sulfides apparently coincides with the tourmaline zone, which is surficially marked by ochreous products of oxidation in which jarosite is abundant. The oxidized zone also contains minute amounts of malachite.

The emerald crystals occur in tourmaline zones and, rarely, in the quartz veins (Fig. 3a). Where quartz veins cut mica-poor schist, there are no tourmaline or sulfide zones, and there is no emerald (although there may be tourmaline in the quartz veins). Thus, we infer that mica-poor strata were relatively unreactive with respect to the hydrothermal system.

One kilometer southeast (and approximately 1.8 km east) of the emerald showing is one of the largest bodies of mid-Cretaceous granite in the area. The pluton is zoned; the part closest to the emerald showing is an apparently near-margin muscovite granite that, over a few tens of meters, grades to more typical reddish-

FIG. 2a. Regional geological map of the area of the Regal Ridge emerald.

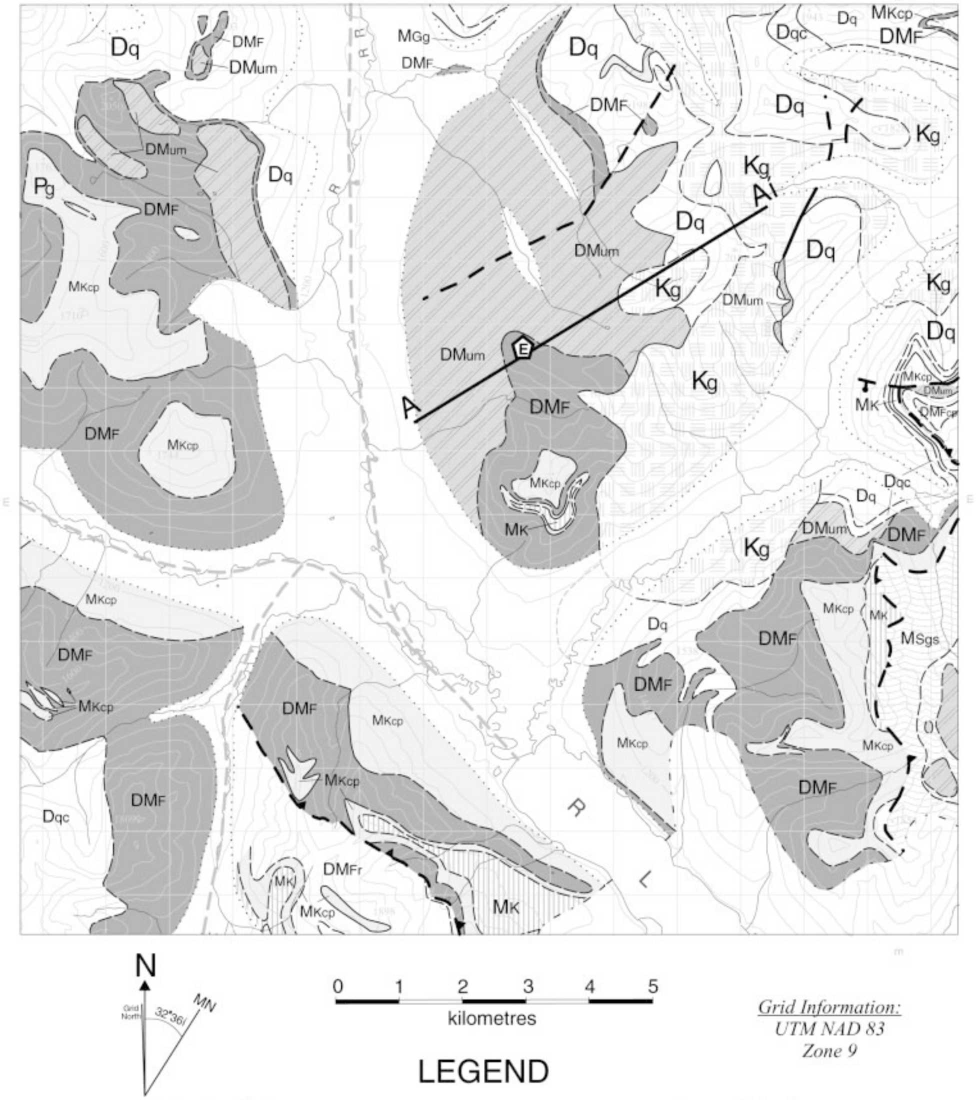

LEGEND

Intrusive Rocks

CRETACEOUS

Kg	weakly foliated biotite-muscovite granite

MISSISSIPPIAN
Simpson Range plutonic suite

MSg	biotite-hornblende granite and quartz monzonite
MSgs	strongly foliated unit MSg

DEVONIAN-MISSISSIPPIAN

DMum	serpentinized ultramafic rock; lesser gabbro and pyroxenite

Ⓔ Crown Emerald Showing

A____Aí line of cross-section

Layered Rocks

MISSISSIPPIAN
Grass Lakes succession

MK	Kudz Ze Kayah felsic meta-volcanic unit: feldspar-muscovite quartz schist of volcanic or volcaniclastic protolith
MKcp	carbonaceous phyllite and grey quartzite

DEVONIAN-MISSISSIPPIAN

DMFcp	carbonaceous phyllite, grey quartzite, pale green chert and grey marble
DMFr	feldspar-muscovite quartz schist of volcanic or volcaniclastic protolith
DMF	Fire Lake mafic meta-volcanic unit: biotite-plagioclase actinolite-chlorite schist (meta-andesite and -basalt)
Dqc	marble and calc-schist
Dq	biotite-muscovite-feldspar-quartz schist, micaceous quartzite and psammite, quartz-biotite-muscovite pelitic schist

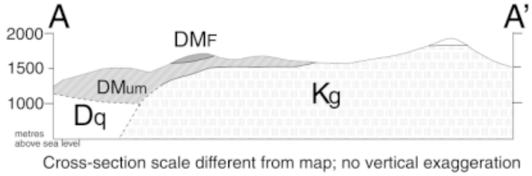

Cross-section scale different from map; no vertical exaggeration

FIG. 2b. Cross-section corresponding to the line A–A' in (a).

weathering biotite–muscovite granite. The granite is weakly foliated, and its contact is discordant with respect to planar fabrics of the host metamorphic rocks, indicating late- to post-kinematic emplacement. A metamorphic aureole exists around the pluton, as shown by the assemblage garnet – hornblende – biotite porphyroblasts in the metamorphic rocks close to the granite. The pluton is cut by numerous quartz veins; however, the possible continuity of these quartz veins and those associated with emerald mineralization is obscured by talus and soil cover. Tourmaline is a common accessory mineral, disseminated throughout the granite and within arrays of quartz veins both in and around the granite. The western contact of the granite is gently west-dipping, and is interpreted to underlie the Regal Ridge showing at a relatively shallow depth. The orientation of the western contact of the granite and of the contact between the Fire Lake unit and the comagmatic mafic and ultramafic sill are such that the granite likely penetrates the ultramafic sill at depth (Fig. 2b). A small (approximately 9 m^2) outcrop of muscovite granite approximately 600 m east of the emerald mineralization is macroscopically identical to the near-margin granite in the pluton.

MINERALOGY

Emerald

The beryl crystals attain 4 cm in length. Some of the smaller crystals, and sections of larger crystals, are gem-quality, with excellent clarity and color. Many of the larger crystals show a regular pattern of cavities (Fig. 3b) that likely represent inclusions that have weathered away. Others crystals appear to have grown across the foliation of the schist, as shown by trains of micaceous inclusions, which create parting planes and increase susceptibility to physical weathering. Twenty-four crystals of emerald were examined from five of the source regions. One additional crystal (sample R) was obtained from a quartz vein on the south side of the ridge, at the westernmost extent of the showing. All samples are green in hand specimen and exhibit a homogeneous distribution of color. A preliminary investigation by scanning electron microscopy, using both back-scattered electron and cathodoluminescence imaging modes, showed no evidence of compositional zoning. A total of 85 electron-microprobe analyses was obtained from the 25 samples (details of the analytical

FIG. 3. (left) Emerald crystal in quartz matrix; the crystal is approximately 4 mm in length. (right) A cluster of emerald crystals, showing cavities. The main crystal is approximately 4 mm in diameter.

procedures are provided in the Appendix). The analytical results were recalculated on the basis of 18 O and three Be atoms per formula unit (*apfu*). It is important to note that this approach gives the maximum possible Be content and ignores possible substitution at the Be site. Results of selected analyses are given in Table 1. The average Cr concentration is 3208 ppm (maximum 7816 ppm), and the mean and maximum V concentrations are 171 and 333 ppm, respectively. Both Cr and V are chromophoric in emerald; however, the concentration of Cr indicates the predominant importance of Cr. Six of the analyses show Cr concentrations of <1000 ppm (1 to 761 ppm); five of these are from crystal rims, and one is from an intermediate area between the core and rim of a crystal. The Fe content is variable between relatively narrow limits (0.02 to 0.05 *apfu*), particularly if compared to the Mg concentrations, which range between 0.08 and 0.18 *apfu.* Some of the crystals contain significant concentrations of Sc (up to 499 ppm).

Figure 4a shows Al *versus* the sum of other *Y* site (octahedral) cations; as expected, they show an inverse relationship. The samples with the highest Al contents are generally from areas 4 and R. In Figure 4b, the compositions from this study are plotted with those from the literature. Most of the Regal Ridge material falls in the middle of the range, and there is little overlap with data from the literature except at the Al-rich end (Al > 1.85 *apfu*). The most Al-rich compositions pertain to samples from the Muzo and Somondoco regions of Colombia. These deposits are unique in that they are hosted by black shales and originate from evolved sedimentary brines (Giuliani *et al.* 1995, Sabot *et al.* 2001). The most Al-poor samples are from schists in the Swat and Mohmand districts of Pakistan, where the deposits are associated with an oceanic suture zone (Lawrence *et al.* 1989), and from the Ankadilalana mine in Madagascar, where the emerald occurs in the contact zone between pegmatites and biotite schist (Hanni & Klein 1982).

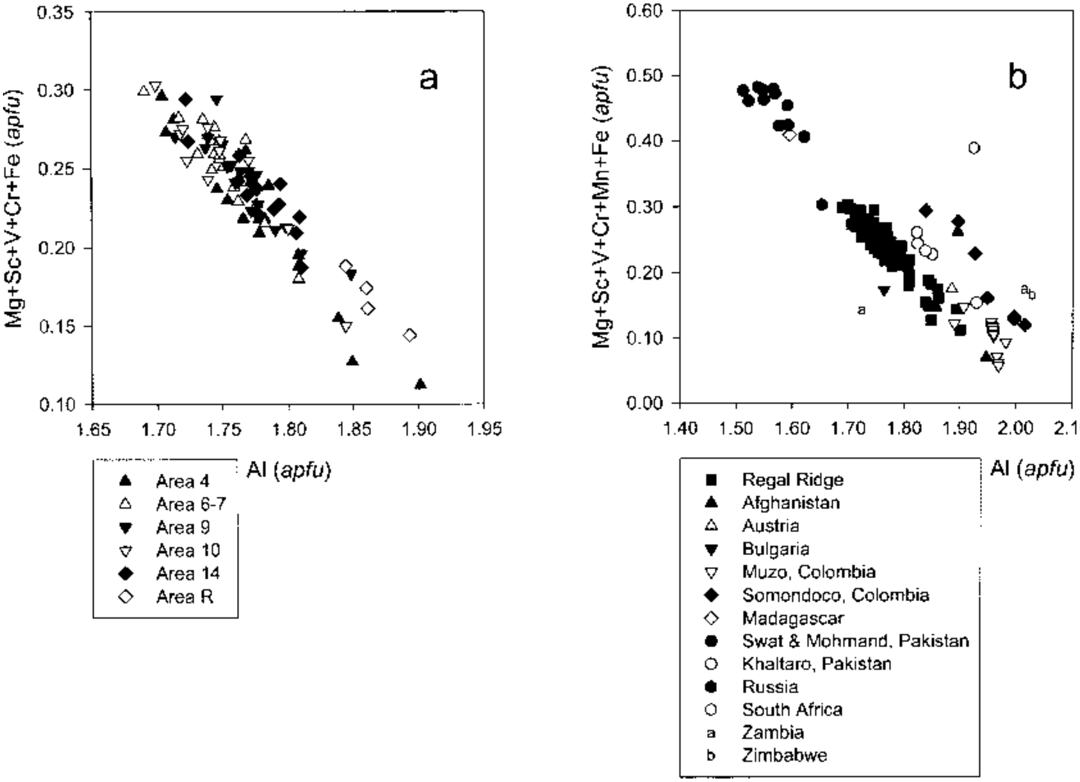

FIG. 4. Al *versus* the sum of other *Y*-site cations, in atoms per formula unit, for (a) samples from this study, and (b) samples from this study and from the literature. Sources of data: Kovaloff (1928), Zambonini & Caglioto (1928), Leitmeier (1937), Otero Muñoz & Barriga Villalba (1948), Gübelin (1958), Vlasov & Kutakova (1960), Martin (1962), Petrusenko *et al.* (1966), Beus & Mineev (1972), Hickman (1972), Hanni & Klein (1982), Graziani *et al.* (1983), Kozlowski *et al.* (1988), Hammarstrom (1989), and Ottaway (1991).

Figure 5a shows a nearly 1:1 correlation between Mg + Fe and the sum of monovalent cations. As Mg and Fe are the most abundant of the cations likely to substitute for Al in the beryl structure, this graph suggests that, to achieve charge balance, the substitution of Mg + Fe^{2+} for Al in the *Y* site is coupled with the substitution of a monovalent cation for a vacancy in the channel site. The majority of points lies slightly to the right of the 1:1 line, likely because some of the Fe is present as Fe^{3+}. Why the points representing sample 9 lie well below the 1:1 line is unclear; possibilities include Li substitution for vacancies in the channel sites. The samples with the highest contents of Mg + Fe and monovalent cations are from areas 6–7 and 10; those with the lowest values are from areas 4 and R. In Figure 5b, the compositions are plotted with those from the literature. The Regal Ridge material overlaps the composition of a sample from a pegmatite that intruded amphibolites and hornblende-mica schists at Khaltaro, Pakistan (Hammarstrom 1989) and, to some extent, that of samples from Somondoco, Colombia.

The main substituents for Al at the *Y* site are plotted as oxides in Figure 6a. Most of the variation is between Mg and Cr, whereas the FeO content remains relatively constant. Corresponding values from other deposits are shown in Figure 6b.

TABLE 1 SELECTED ELECTRON-MICROPROBE COMPOSITIONS OF EMERALD FROM THE REGAL RIDGE SHOWING, YUKON TERRITORY

Sample	4-4 Rim	14-4 Rim	6-7-2 Core	4-4 Rim	10-3 Core	4-5 Rim	4-1 Rim	4-5 Rim
SiO_2 (wt.%)	64.98	63.88	63.98	64.55	63.83	64.09	64.46	65.44
Al_2O_3	17.52	16.06	15.79	15.65	15.34	16.25	15.55	17.10
Sc_2O_3	0.01	**0.08**	0.06	0.03	0.00	0.04	0.02	0.01
V_2O_3	0.02	0.04	**0.05**	0.02	0.00	0.02	0.02	0.02
Cr_2O_3	0.00	0.45	0.45	**1.14**	0.41	0.36	0.52	0.01
BeO*	13.56	13.32	13.34	13.43	13.27	13.38	13.41	13.60
MgO	0.61	1.16	1.35	1.12	**1.69**	1.15	1.54	0.65
CaO	0.01	0.02	0.03	0.02	**0.07**	0.02	0.04	0.02
FeO	0.33	0.44	0.47	0.50	0.46	**0.61**	0.54	0.45
Na_2O	0.65	1.02	1.09	1.00	1.18	0.99	**1.25**	0.78
K_2O	0.02	0.02	0.02	0.03	0.00	0.01	0.03	0.01
Cs_2O	0.07	0.15	0.11	0.15	0.07	0.16	0.12	**0.22**
H_2O	2.07	1.18	1.91	2.07	1.98	2.07	2.07	2.07
Total	99.85	97.82	98.64	99.71	98.30	99.15	99.57	100.38
Si^{4+} (*apfu*)	5.986	5.989	5.995	6.002	6.006	5.984	5.980	6.010
Al^{3+}	**1.902**	1.775	1.744	1.715	1.701	1.788	1.770	1.851
Sc^{3+}	0.001	**0.007**	0.005	0.002	0.000	0.003	0.001	0.001
V^{3+}	0.001	0.003	**0.004**	0.001	0.000	0.001	0.001	0.001
Cr^{3+}	0.000	0.033	0.033	**0.084**	0.031	0.027	0.036	0.001
Be^{2+}	3.000	3.000	3.000	3.000	3.000	3.000	3.000	3.000
Mg^{2+}	0.084	0.162	0.189	0.155	**0.237**	0.160	0.190	0.089
Ca^{2+}	0.001	0.002	0.003	0.002	**0.007**	0.002	0.004	0.002
Fe^{2+}	0.025	0.034	0.037	0.039	0.036	**0.048**	0.034	0.035
Na^+	0.116	0.185	0.198	0.180	0.215	0.179	**0.226**	0.139
K^+	0.002	0.002	0.002	0.004	0.000	0.001	0.004	0.001
Cs^+	0.003	0.006	0.004	0.006	0.003	0.006	0.005	**0.009**
H^+	0.64	0.37	0.60	0.64	0.62	0.64	0.64	0.63
Sc (ppm)	71	**499**	380	191	57	234	62	39
V	135	300	**333**	137	82	169	111	120
Cr	1	3076	3094	**7816**	2773	2456	3364	92
Cs	680	1371	1045	1368	520	1491	594	**2100**

Note: Compositions were recalculated on the basis of 3 Be and 18 O *apfu*. H_2O is by step-heating and quadropolar mass spectrometry except for the 14-4 Rim value, which is a minimum estimate based on two H_2O molecules per Na *apfu*. Maximum values are shown in bold.

*Determined by stoichiometry.

The elements responsible for most of the variation in color in emerald crystals are plotted as oxides in Figure 7a, and corresponding values from other deposits are shown in Figure 7b. In most cases, the Cr_2O_3 content is much greater than that of V_2O_3; the main exceptions are for samples from Muzo, Colombia.

Cell dimensions, optical data and density data show little variation (Table 2). The *a* cell parameters vary from 9.232 to 9.243 Å, and *c* ranges from 9.196 to 9.205 Å. The *c*/*a* values (0.995–0.996) show that these samples consist of beryl in which Al ↔ Me^{2+} represents the main isomorphous replacement (Aurisicchio *et al.* 1988). The indices of refraction n_e and n_o vary from 1.571 to 1.586, and from 1.578 to 1.586, respectively. These are near the low end of the values listed by Gübelin (1989) for emerald crystals from many deposits (n_e 1.569 to 1.592, n_o 1.576 to 1.602). Measured densities range from 2.678 to 2.726 g/cm^3.

Investigation of polished mounts with the SEM revealed the presence of cavities in some samples, up to 0.75 mm in diameter (Fig. 8); accessory minerals within these cavities include chromite, ferberite or ferritungstite, hematite, a mineral of the jarosite group, and scheelite. The SEM study also revealed an abundance of solid and fluid inclusions; the former include calcite, chalcopyrite, molybdenite, phlogopite, pyrite, quartz, tourmaline, and zircon (Fig. 8). Electron-microprobe data for the phlogopite inclusions in emerald are given in Table 3. The *X*-site totals are low, possibly because the inclusions are only 20 to 30 μm across and have irregular surfaces. The phlogopite has moderate Cr (to 0.02 Cr *apfu*) and high F (to 1.139 *apfu*) contents.

Tourmaline

A tourmaline-group mineral is ubiquitous and abundant in the area of the Regal Ridge showing. The mineral is present in the granite, in the quartz veins, as large, discrete crystals in the schist, and is associated with the emerald mineralization as masses of fine crystals that surround the quartz veins where they cut the mica-rich parts of the schist. Tourmaline needles also occur as inclusions in many of the emerald crystals. Selected

TABLE 2. PHYSICAL PROPERTIES OF EMERALDS FROM THE REGAL RIDGE SHOWING, YUKON TERRITORY

Crystal	Cell Dimensions (Å)			Indices of Refraction		D_{meas}
	a (Å)	*c* (Å)	*V* ($Å^3$)	n_e	n_o	
4-2 small	9.2397(7)	9.2023(8)	680.4(1)	-	-	2.726
4-2 medium	9.243(1)	9.201(1)	680.7(2)	1.571	1.578	2.708
4-2 large	9.2383(7)	9.1983(6)	679.9(1)	1.578	1.584	-
4-4	9.2315(7)	9.1972(8)	678.8(1)	1.571	1.579	2.705
6-7-1 small	9.2353(8)	9.1964(8)	679.3(1)	1.571	1.579	2.719
6-7-1 large	9.232(2)	9.195(2)	678.6(5)	1.576	1.584	2.709
6-7-2	9.2414(4)	9.1999(5)	680.44(7)	1.576	1.582	2.693
9-4	9.242(1)	9.2008(7)	680.6(1)	1.578	1.586	2.693
14-2 small	9.2376(8)	9.2052(9)	680.3(1)	1.571	1.579	2.678
14-2 large	9.232(2)	9.197(2)	679.2(4)	1.571	1.579	2.705

electron-microprobe compositions are given in Table 4. The tourmaline ranges in composition from dravite to uvite. Most of the tourmaline within the schist, but distal from the quartz veins, is schorl to dravite in composition (Figs. 9a, b). The fine-grained crystals that surround the quartz veins are dominantly dravite, whereas the tourmaline inclusions in emerald are dravite to uvite in composition. In general, the tourmaline compositions show increasing Ca and Mg (at the expense of Na + vacancies and Fe, respectively) with proximity to the emerald mineralization.

The presence of tourmaline may be a key to understanding the absence of a high concentration of Fe in the beryl (which would tend to attenuate the emerald-green color); under high B activity, tourmaline acts as a sink for Fe, Mg and Mn.

Other minerals

The crumbly yellow sulfate-rich material associated with the quartz veins was sieved, and the fine powder

TABLE 3 ELECTRON MICROPROBE COMPOSITIONS OF PHLOGOPITE INCLUSIONS IN EMERALD, REGAL RIDGE SHOWING, YUKON TERRITORY

Sample	10-3	9-2	9-3		10-3	9-2	9-3
SiO_2 (wt.%)	41.44	41.00	42.57	Si^{4+} (*apfu*)	3.018	3.027	3.073
TiO_2	0.29	0.20	0.26	Ti^{4+}	0.016	0.011	0.014
Al_2O_3	12.81	11.89	12.17	Al^{3+}	1.100	1.035	1.035
V_2O_3	0.02	0.02	0.06	V^{3+}	0.001	0.001	0.003
Cr_2O_3	0.16	0.24	0.39	Cr^{3+}	0.009	0.014	0.022
MgO	22.33	22.33	22.04	Mg^{2+}	2.425	2.458	2.372
MnO	0.23	0.22	0.19	Mn^{2+}	0.014	0.014	0.012
FeO	6.21	6.55	6.54	Fe^{2+}	0.378	0.404	0.395
BaO	0.08	0.04	0.04	Ba^{2+}	0.002	0.001	0.001
Na_2O	0.13	0.37	0.36	Na^+	0.018	0.053	0.050
K_2O	9.33	9.35	9.23	K^+	0.867	0.881	0.850
Rb_2O	0.12	0.13	0.11	Rb^+	0.006	0.006	0.005
Cs_2O	0.10	0.07	0.09	Cs^+	0.003	0.002	0.003
H_2O*	2.17	1.79	1.79	H^+	1.056	0.881	0.861
F	4.10	4.79	4.99	F^-	0.944	1.119	1.139
O=F	-1.73	-2.02	-2.10	O^{2-}	11.056	10.881	10.861
Total	97.80	96.97	98.73				

Note: Compositions were recalculated on the basis of 12 (OH, F) *apfu*. The 9-2 values are the average of two analyses.
*Determined by stoichiometry, assuming 2 (OH, F) *apfu*.

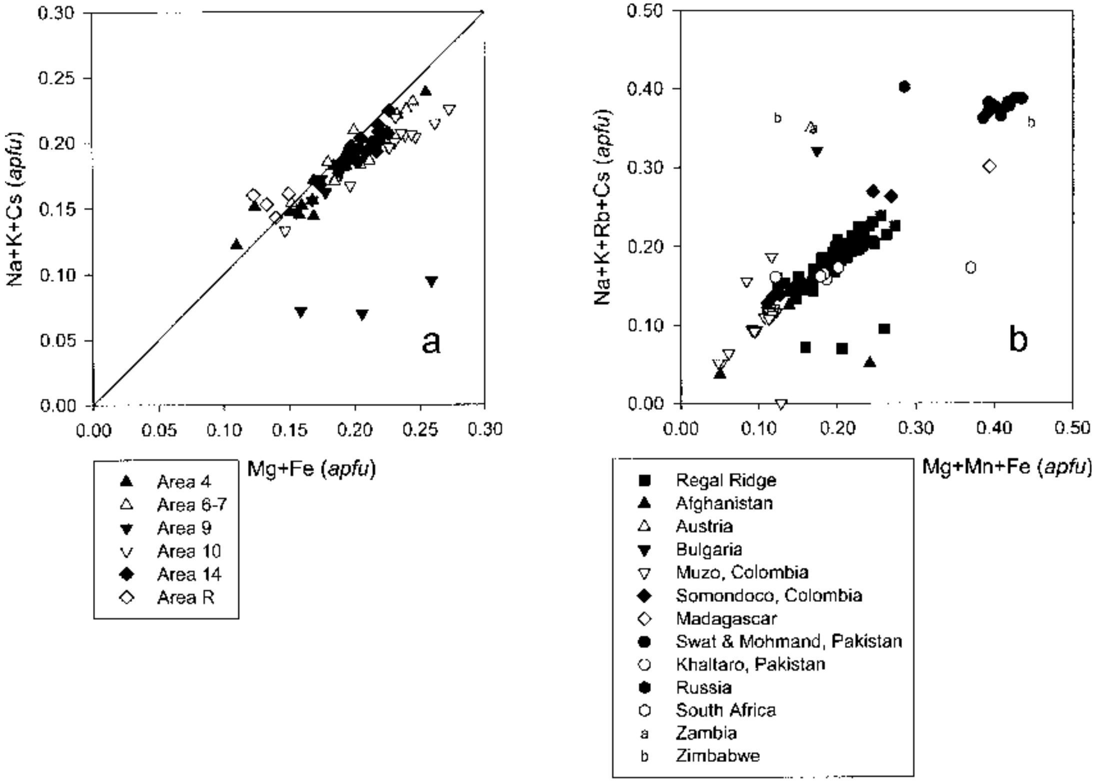

FIG. 5. (a) Mg + Fe *versus* the sum of monovalent channel-site cations, in atoms per formula unit, for samples from this study. (b) Mg + Mn + Fe *versus* monovalent channel-site cations for samples from the literature. Sources of data are the same as in Figure 4b. The 1:1 line has been omitted for clarity.

was analyzed by X-ray diffraction. The X-ray spectra show a mixture of jarosite, chlorite, and mica. Gypsum is commonly present as thin layers on rocks in the talus below the ridge. The source of the sulfur is likely the sulfide minerals associated with the quartz veins and the tourmaline zone. However, it is also possible that there is a significant amount of syngenetic sulfide mineralization in the mafic schists. Pyrite and, less commonly, chalcopyrite occur disseminated throughout the unit regionally and are locally concentrated into millimeter- to centimeter-scale seams.

As noted previously, scheelite crystals occur locally within the tourmaline zone near the quartz veins. The presence of scheelite rather than ferberite is probably

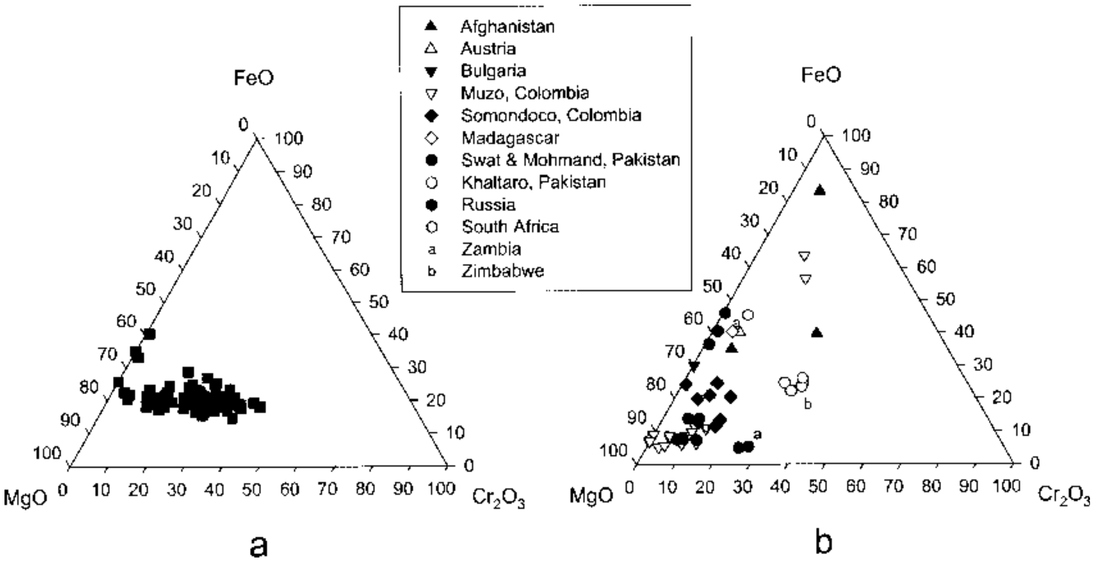

FIG. 6. Plot of emerald compositions in terms of FeO–MgO–Cr_2O_3 (wt.%). Data from (a) this study, and (b) from the literature (with all Fe as FeO). Sources of data are the same as in Figure 4b. The diagrams are after Hammarstrom (1989).

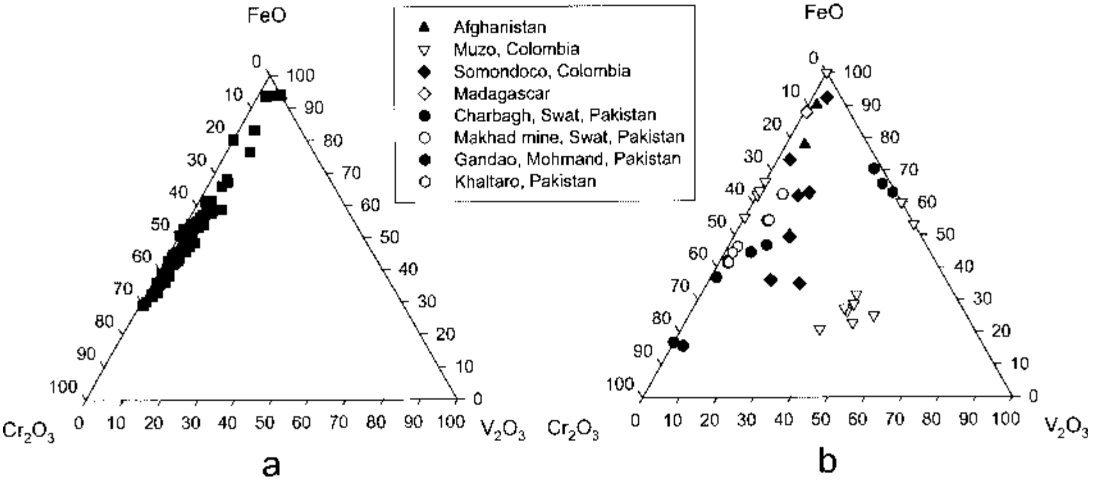

FIG. 7. Plot of emerald compositions in terms of FeO–Cr_2O_3–V_2O_3 (wt.%). Data from (a) this study, and (b) from the literature (with all Fe as FeO). Sources of data are the same as in Figure 4b. The diagrams are after Hammarstrom (1989).

related to the scavenging properties of tourmaline as regards Fe and Mn, and to the presence of moderately calcic host-rocks. Marble lenses occur locally in the host rocks, and pockets containing very pale beryl have been found encapsulated in hydrothermal calcite. Numerous examples of beryl in association with tungsten minerals are reported in the literature. However, the only tungsten-enriched emerald deposits known are the Regal Ridge showing and those in phlogopite associated with the Campo Formoso and Carnaiba granites in Brazil (Rudowski *et al.* 1987).

FLUID INCLUSIONS

Primary and pseudosecondary fluid inclusions occur in the emerald (Marshall *et al.* 2002). The fluid inclusions contain three fluid phases at room temperature. The dominant phase is an aqueous brine occupying approximately 80% of the fluid-inclusion volume. The other two phases are gaseous and liquid carbonic fluids, representing approximately 4 and 16% of the volume, respectively. Although there is clear evidence of necking-down (Roedder 1984), many of the inclusions display a consistent ratio of phases, thus suggesting a single population. Accidental inclusions that have been observed within the fluid inclusions are of a transparent birefringent micaceous mineral. This is probably phlogopite and is consistent with the SEM studies. No daughter minerals were observed within the fluid inclusions during microthermometric measurements (Marshall *et al.* 2002). The microthermometric measurements of 42 fluid inclusions indicate that the carbonic phases are dominated by CO_2 but contain minor amounts of dissolved methane; $X(CH_4)$ (equivalent) in the gaseous phase attains 0.15. Raman studies have been ineffective because the emerald fluoresces, thereby overprinting any signal from the gases. Temperatures of clathrate melting indicate that the emerald precipitated from a fluid whose maximum salinities were 3 wt.% NaCl equivalent. SEM–EDS observation of breached fluid-inclusion surfaces failed to show any residua containing cations commonly associated with saline fluid inclusions; thus, the salinities are reported as NaCl equivalent. The fluid-inclusion compositions were approximated from the microthermometry by using a pseudoternary (H_2O–CO_2–NaCl) system with an $X(CH_4)$ of 0.1, utilizing the data of Diamond (1992) and the techniques of Diamond (2001) and Bakker & Diamond (2002). This yielded an estimated fluid composition of 0.9391 mole % H_2O, 0.0473 mole % CO_2, 0.0077 mole % CH_4, 0.0059 mole % NaCl (~2 wt.% NaCl eq.), and an estimated bulk molar volume of 26.35 cm^3/mol (Marshall *et al.* 2002). Isochores based on the fluid compositions were calculated using the GASWET program of Bakker (1999) and were checked against an extrapolation of the experimental data of Gehrig (1980).

TABLE 4 SELECTED ELECTRON MICROPROBE COMPOSITIONS OF TOURMALINE FROM THE REGAL RIDGE SHOWING, YUKON TERRITORY

Sample	4-7 Host rock	1-4 Host rock	3-4 Tur zone	3-5 Tur zone	14/4 Inclusion	14/2 Inclusion	2-4 Host rock
SiO_2 (wt %)	**37.42**	34.59	36.11	35.72	35.11	35.76	35.69
TiO_2	0.28	**1.56**	0.21	0.31	0.17	0.21	0.41
SiO_2	**37.42**	34.59	36.11	35.72	35.11	35.76	35.69
B_2O_3*	10.58	10.27	**10.65**	10.62	10.32	10.51	10.61
Al_2O_3	28.23	30.96	29.32	**33.75**	28.68	28.09	32.73
Cr_2O_3	0.11	0.01	0.06	0.05	**3.28**	0.18	0.20
MgO	9.76	4.80	**12.17**	7.95	8.49	11.91	8.40
CaO	2.78	0.75	3.01	1.53	1.99	**3.39**	1.29
MnO	0.00	**0.31**	0.02	0.00	0.07	0.05	0.02
FeO	6.95	**10.69**	3.46	4.83	5.68	4.51	5.18
Na_2O	1.63	**2.16**	1.26	1.19	1.56	1.10	1.70
K_2O	0.01	**0.06**	0.02	0.02	0.02	0.00	0.02
H_2O*	3.53	3.11	3.32	3.57	3.27	2.97	**3.65**
F	0.25	0.91	0.76	0.19	0.61	**1.38**	0.02
O=F	-0.11	-0.38	-0.32	-0.08	-0.26	-0.58	-0.01
Total	101.43	99.80	100.07	99.65	99.00	99.49	99.92
Si^{4+} (*apfu*)	**6.144**	5.855	5.891	5.845	5.911	5.912	5.844
Ti^{4+}	0.035	**0.199**	0.026	0.038	0.022	0.026	0.050
B^{3+}	3.000	3.000	3.000	3.000	3.000	3.000	3.000
Al^{3+}	5.463	6.176	5.638	6.509	5.691	5.473	6.317
Cr^{3+}	0.014	0.001	0.008	0.006	**0.437**	0.024	0.026
Mg^{2+}	2.389	1.211	**2.960**	1.939	2.131	2.935	2.051
Ca^{2+}	0.489	0.136	0.526	0.268	0.359	**0.600**	0.226
Mn^{2+}	0.000	**0.044**	0.003	0.000	0.010	0.007	0.003
Fe^{2+}	0.954	**1.513**	0.475	0.661	0.800	0.624	0.709
Na^+	0.519	**0.709**	0.399	0.378	0.509	0.353	0.540
K^+	0.002	**0.013**	0.004	0.004	0.004	0.000	0.004
H^+	3.870	3.513	3.608	3.902	3.675	3.278	**3.990**
F^-	0.130	0.487	0.392	0.098	0.325	**0.722**	0.010
O^{2-}	31.038	30.652	30.575	31.002	30.787	30.241	31.054

Note. Compositions were recalculated on the basis of 15 (Mg^{2+}, Mn^{2+}, Fe^{2+}, Al^{3+}, Cr^{3+}, Si^{4+}, Ti^{4+}) *apfu*. Maximum values are shown in bold.
*Determined by stoichiometry, assuming 4 B *apfu* and 2 (OH, F) *apfu*.

The low salinities are unusual, although Seal (1989) reported values of about nil to approximately 20 wt.% dissolved salts for fluid inclusions hosted by emerald from the Swat district in Pakistan. In addition, Giuliani *et al.* (1997a) reported salinites of 1 to 22 wt.% for fluid inclusions in emerald from the Santa Terezinha de Goiás deposit in Brazil. Both deposits are associated with tectonic structures and are not directly associated with granitic intrusions. However, low-salinity H_2O–CO_2–NaCl-bearing fluid inclusions have been observed in emerald from the Gravelotte (South Africa; Nwe & Morteani 1993), Franqueira (Spain; Martin-Izard *et al.* 1995, Fuertes-Fuente *et al.* 2000), Sumbawanga and Lake Manyara (Tanzania; Moroz & Vapnik 1999), Malysheva (Russia; Moroz & Vapnik 1999), and Rila localities (Bulgaria; Alexandrov *et al.* 2001); all are schist-type deposits with associated pegmatites. The maximum salinity recorded for this type of deposit is 37 wt.% NaCl equivalent (Brazil; Barros & Kinnaird 1985). Fluid inclusions in Colombian (Ottaway 1991, Giuliani *et al.* 1992, Kozlowski *et al.* 1988, Ottaway *et al.* 1994, Banks *et al.* 2000) and Afghani emerald (Seal 1989, Moroz & Vapnik 2001) have higher salinities (>38 wt.% NaCl equivalent), which result from the dissolution of evaporites by hydrothermal fluids (Giuliani *et al.* 1995, Sabot *et al.* 2001).

STABLE ISOTOPES

Aines & Rossman (1984) showed that when heated above 400°C, and after liberation of fluid inclusions, the H_2O in beryl partitions into an unbound state as gaseous molecules confined to the channel voids. Brown & Mills (1986) showed that the channel H_2O is liberated at temperatures of ~800°C, and Taylor *et al.* (1992) reported that isotopic fractionation seems to be minimal during dehydration. Thus, channel H_2O may represent the original fluid from the time of formation, and the measurement of δD in H_2O released from beryl may then permit determination of the source of the fluids from which the beryl grew. Such investigations have been applied successfully to beryl from a number of deposits (Fallick & Barros 1987, Taylor *et al.* 1992, Arif *et al.* 1996, Giuliani *et al.* 1997a). The hydrogen isotopic composition of channel H_2O from the samples of Regal Ridge emerald falls within a narrow range between –62.1 and –57.3‰ (Table 5). The measured δD values are consistent with both a magmatic and a metamorphic origin for the fluids (Fig. 10). The total H_2O content in the channels is between 1.91 and 2.07 wt.% H_2O (Table 5) and falls within the range defined for beryl from granitic pegmatites ($1.2 < H_2O^+ < 2.55$ wt.%; Taylor *et al.* 1992) and emerald from a variety of geological environments ($0.83 < H_2O^+ < 3.33$ wt.%; Giuliani *et al.* 1997a, 1998; Table 6).

The oxygen isotopic composition, obtained from seven samples, is highly variable (Table 5). The $\delta^{18}O$ values are very different from those of hydrothermally grown synthetic emerald, and from beryl in pegmatites and pegmatite-related emerald deposits (Tables 6, 7). The values are within the range defined for Afghani

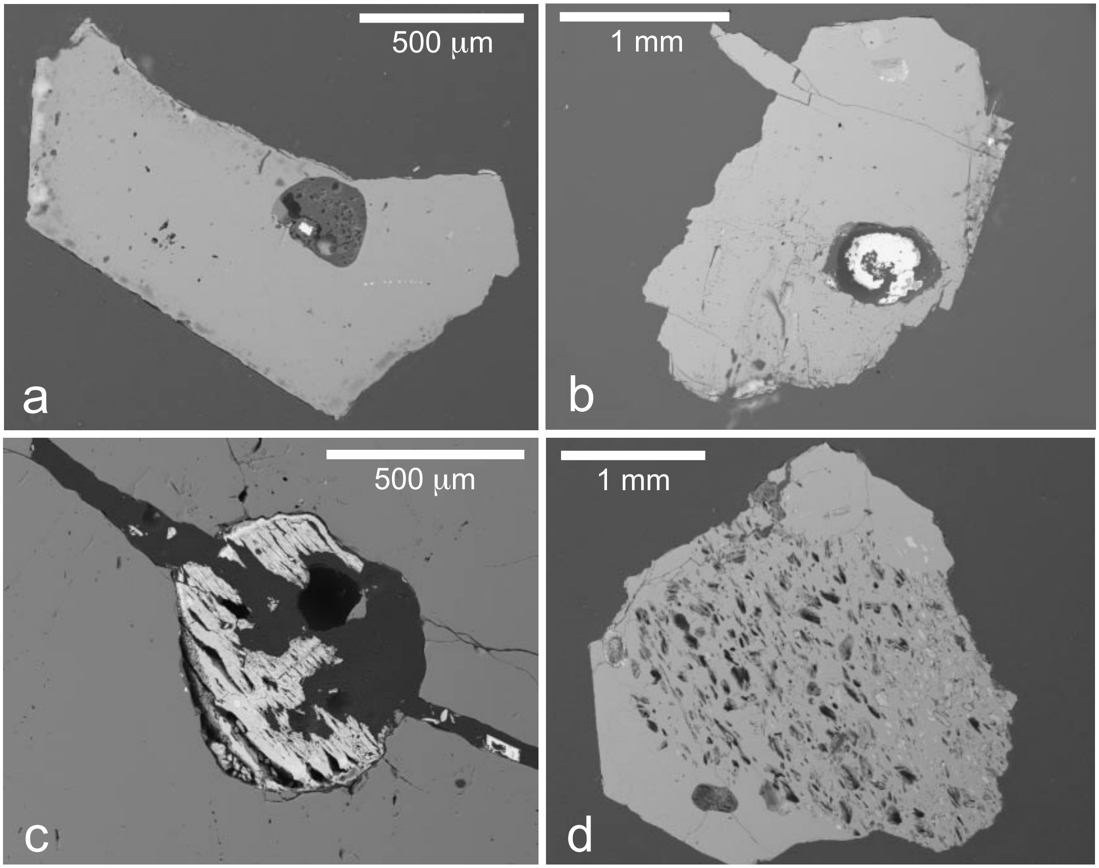

FIG. 8. Back-scattered electron (BSE) images of emerald samples, showing a variety of inclusions: (a) sample 4–5, showing a hole containing a chalcopyrite crystal; (b) sample 6–7, a hole containing ferberite or ferritungstite; (c) sample 14–4, ferberite or ferritungstite in a fracture; (d) sample 9–3, representative of the high density of inclusions in samples from Area 9; (e) sample 4–2, showing tourmaline inclusions; (f) sample 9–2, with phlogopite and tourmaline inclusions; (g) sample 10–3, showing inclusions of molybdenite and zircon.

(Panjsher Valley) emerald ($\delta^{18}O = 13.5 \pm 0.1‰$) and the Brazilian Santa Terezinha deposit ($\delta^{18}O = 12.2 \pm 0.1‰$) (Table 7). Both are shear-zone-related deposits that are not genetically linked to granites.

The $\delta^{18}O$ values for emerald vary from 12.3‰ for samples 6–7–1 and 6–7–3 to 14.8‰ for sample 4–4 (Table 5); however, there is little difference in δD values (–57.3 and –59.8‰, respectively). These results suggest the presence of an isotopically homogeneous fluid that underwent isotopic exchange with the host rocks during the metasomatic process. The 2.5‰ variation in $\delta^{18}O$ obtained for the emerald shows that homogenization was not achieved and that the fluid was not completely buffered during the fluid–rock interaction.

To investigate a possible link between the nearby Cretaceous granite and the emerald, the isotopic compositions of primary quartz, biotite, and muscovite from the granite were determined. The results (Table 5) show that the micas are highly depleted in D and have slightly enriched ^{18}O values relative to the international SMOW standard. Equilibrium compositions of the magmatic H_2O emanating from the Cretaceous granite, calculated using the calibrations of Bottinga & Javoy (1973, 1975) and Suzuoki & Epstein (1976) over the temperature range 500 to 800°C, are plotted on Figure 11. The calculated compositions of magmatic H_2O for the granite fall outside the boxes for Cornubian and normal magmatic H_2O, indicating that the magmatic H_2O in equilibrium with the granite was depleted in D, or that the samples have been altered and incorporated the highly D-depleted meteoric H_2O typical of northwestern North America. We deem this an unlikely possibility, as care was taken to obtain fresh samples; moreover, the values

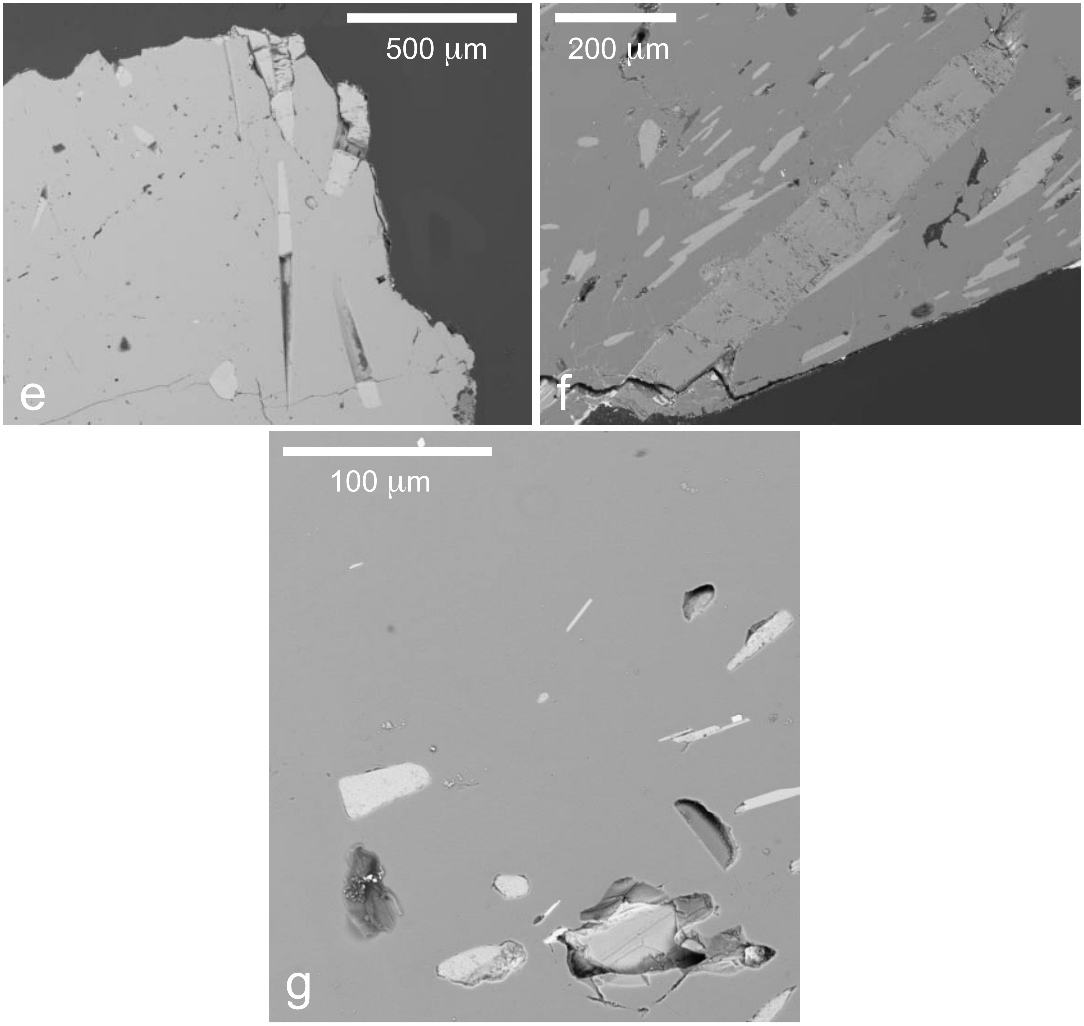

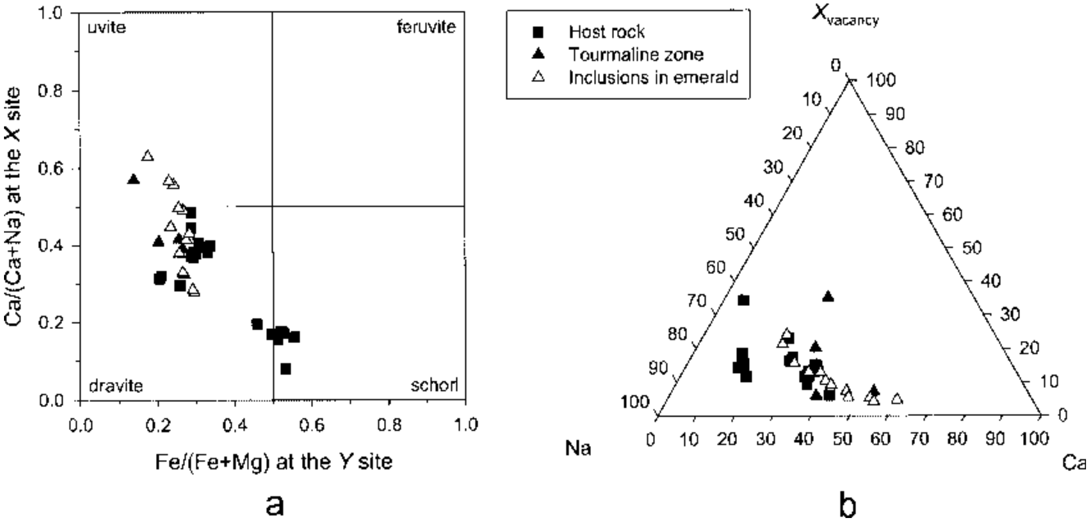

FIG. 9. (a) Diagram of Fe/(Fe + Mg) at the *Y* site *versus* Ca/(Ca + Na) at the *X* site for tourmaline samples from the Regal Ridge showing. (b) Triangular plot of tourmaline samples from the Regal Ridge shown in terms of *X*-site vacancies – Na – Ca.

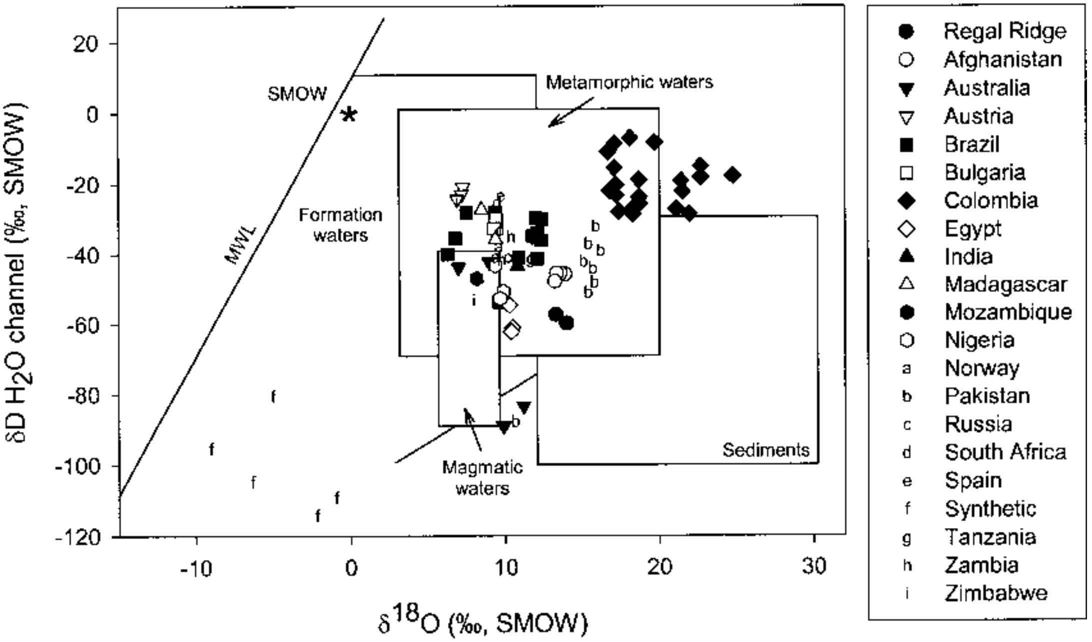

FIG. 10. Hydrogen and oxygen isotopic compositions for emerald samples from the Regal Ridge property, compared to data for synthetic hydrothermally grown emerald and emerald from other localities. The oxygen data are from Giuliani *et al.* (1998) and the hydrogen data are from this work (Table 5) and Giuliani *et al.* (1997a). The isotopic compositional fields are from Sheppard (1986). MWL: Meteoric Water Line, SMOW: Standard Mean Ocean Water.

are in good agreement with those reported for emerald from the Khaltaro deposit in Pakistan.

The $\delta^{18}O$ values for coexisting quartz and tourmaline from quartz veins in the area of emerald mineralization are 12.37, 9.52, and 10.30‰, respectively (Table 5). Based on $\delta^{18}O_{Qtz-Tur}$ values of 2.85 and 2.07, the quartz–tourmaline geothermometer of Kotzer *et al.* (1993) yields temperatures of formation of approximately 365 and 498°C, respectively (Marshall *et al.* 2002). On the basis of fluid-inclusion isochoric data (Marshall *et al.* 2002), these temperatures correspond to pressures of 1.0 to 2.5 kbar, and inferred depths of 3 to 7.7 km.

The $\delta^{18}O$ values for H_2O in equilibrium with emerald were calculated for the temperature ranges given by the fluid-inclusion and quartz–tourmaline oxygen isotope studies. These $\delta^{18}O$ values are plotted against emerald channel-H_2O δD in Figure 10. The results are ambiguous and are consistent with a metamorphic or magmatic origin for the fluids responsible for emerald formation.

GEOCHEMISTRY

Geochemical information on the near-margin muscovite granite within the pluton and on the "outcrop" granite 600 m east of the emerald mineralization is given in Table 8. The close proximity to the emerald showing suggests that the granite is the source of the Be. The Be content of the "main" and "outcrop" granites are 13.2 and 12 ppm, respectively (Table 8). This may seem low, but the crustal abundance of Be is <5 ppm, as estimated by Wedepohl (1978), or <3.5 ppm according to Beus (1966), and the range for granites given by Goldschmidt (1954) is 2–20 ppm. The results show that the "outcrop" granite is rich in W (231 ppm), whereas the "main" granite has only 7 ppm W. Both are impoverished in Eu and Lu, which is typical of an evolved S-type granitic system. Both are rich in Li (97 ppm "main", 148 ppm "outcrop"), B (42 ppm "main", 75 ppm "outcrop"), and F (1010 ppm "main", 630 ppm "outcrop"). The high F content is interesting, as Renders & Anderson (1987) have shown that Be is transported in hydrothermal fluids as hydroxyl-, chloride-, or fluoride complexes.

Two samples of quartz from the veins associated with the emerald mineralization were analyzed for Be, F, and W. The results are <0.5 and 29.9 ppm Be, 20 and 150 ppm F, and 2 and 25 ppm W.

The source of the Cr apparently is the boninitic schist; analyses gave Cr and V contents of 520 and 136 to 190 ppm, respectively (Table 9). Boninites are characterized by very high contents of compatible transition metals (*e.g.,* Crawford *et al.* 1989), and those from the Fire Lake unit have much higher contents of Ni, Cr, Sc, and V than other mafic rocks in the Fire Lake unit (Fig. 12; Piercey 2001, Piercey *et al.* 1999, 2001). The serpentinized mafic and ultramafic rocks that outcrop ~0.3–0.5 km away and underlie the showing (Fig. 2) are also likely to be rich in Cr.

The Regal Ridge showing is also rich in W, as shown by the presence of scheelite, and the emerald locally contains inclusions of tourmaline, molybdenite, and chalcopyrite. In the Finlayson Lake area, the 112 Ma granites show a regional association with anomalies in W (and, in some cases, Mo), among which are several occurrences of W skarn (Yukon MINFILE occurrences 105G/018, /019, /020, /039, /071; www.geology.gov.yk.ca/minfile/index.html). Also, many of the granites contain tourmaline as an accessory mineral. Granites in the Finlayson Lake area are moderately to strongly peraluminous and form part of the Anvil plutonic suite (Mortensen *et al.* 2000), a 112–100 Ma suite of peraluminous, felsic intrusions in southern and central Yukon. The offset extension of the Anvil suite into Alaska (on the southwest side of the Tintina Fault) comprises dominantly peraluminous intrusions that yield the same range of crystallization ages as the Anvil suite (Mortensen *et al.* 2000), and are spatially and genetically associated with a large number of W, Mo, Au, and Bi occurrences.

TABLE 5. STABLE ISOTOPE DATA, REGAL RIDGE SHOWING, YUKON TERRITORY

Sample	$\delta^{18}O$ (‰, SMOW)	δD (‰, SMOW)	H_2O channel (wt.%)
Emerald			
4		-59.8	2.07
6-7		-57.3	1.91
9		-61.9	1.97
10		-62.1	1.98
4-3*	14.4(8)†		
4-4 (light green area)	14.8(4)†		
4-4 (green area)	13.9(4)†		
4-5 (light green area)	13.1(3)†		
4-5 (green area)	14.0(7)†		
4 Average	14.0(7)		
6-7-1	12.3(4)†		
6-7-2	14.15(80)‡		
6-7-3	12.3(4)†		
6-7-5	14.5		
6-7 Average	13.1(10)		
Mineralized zone			
quartz	12.4		
scheelite	6.1		
	6.3		
tourmaline	9.5		
	10.3		
Granite outcrop			
biotite	8.6	-117	
muscovite	10.4	-92	
quartz	12.9		

*Sample numbers refer to subsamples of 4 and 6-7.
†Average of two analyses.
‡Average of three analyses.

TABLE 6. STABLE ISOTOPE AND H_2O DATA FOR NATURAL AND SYNTHETIC EMERALD

Country	Locality or source	Sample	$\delta^{18}O$ ‰ SMOW	δD channel ‰ SMOW	H_2O channel wt.%*
NATURAL EMERALD					
AMERICAS					
Brazil	Capoeirana	CAP14	6.3	–40.0	2.57
	Carnaiba	CAJ1	9.6	–53.7	2 47
	Coqui	CO1	12.1	–41.3	2.40
	Itaberai	ITA8	12.1	–35 4	3.18
	Juca	JU7	6.8	–35.5	1.23
	Pela Ema	PE1	11.8	–34.8	2.88
	Pirenópolis	PIR13	9.4	–28	3.01
	Pombos	PO1	7.5	–28.1	2.78
	Santa Terezinha	STA23–1	12.4	–36.1	3.13
		STA23	12.0	–29.8	2.90
		STA24–2	12.4	–30.0	2.95
		STA24–1	12.1	–34.0	3.00
	Socotó	SO18	10.9	–41.0	2.53
Canada	Regal Ridge	4	14.0	–59.8	2.07
		6–7	13.3	–57.3	1.91
Colombia					
Eastern Zone	Oriente	G118	18.3	–28.8	1.39
		G118	18.3	–27.0	1.32
	Klein	G138	17 2	–20.3	1.50
		G138	17.2	–23.2	1.55
	Palo Aranado	G134	17 1	–15.5	1.34
		G134	17.1	–8.7	1.26
	Guala	G136	16.8	–21.9	1.37
	Guali	G125	16.65	–11.0	1 62
	Vega	G101–1	18.1	–7.1	1.33
	El Pulpito	95–36	17.4	–27.9	1.31
Western Zone	Pava	G89	18.7	–25 7	1.44
		G89	18.7	–18.9	1.61
	Cincho	G135	22.7	–18.2	1.63
		G135	22.7	–15.0	1.55
	Coscuez	G119	24.75	–17.7	1.94
	Yacopi	G88A	21.4	–19.2	1.89
		G88C	21.5	–22.2	1.80
	Tequendama	G137	21.95	–28.6	1.89
	Penas Blancas	95–17	19.7	–8.4	1.96
	Guaquimay	95–35	21.1	–27.2	1.64
	Repolal	95–41	18 7	–23.8	1.31
AFRICA					
Egypt	Sikait	EGYP–1	10.3	–54.6	3.13
		EGYP–2	10.5	–61.0	2 77
		EGYP–3	10.4	–62.2	
Madagascar	Morafeno	MAD–1	9.4	–35.8	2.65
		MAD–2	8.5	–27.3	
Mozambique	Maria mine	MA–1	8.2	–47 0	2.25
Nigeria	Kaduna	Ni–1	9.9	–50.7	0.97
		Ni–2	9.4	–43.3	0.89
		Ni–3	9.7	–52 7	0.94
South Africa	Leydsdorp	COBRA–1	9.5	–25.3	2.45
		LEY–1	9.7	–33.1	2.30
NATURAL EMERALD					
Tanzania	Sumbawanga	TAN–1	11.7	–41.3	0.84
Zambia	Miku	ZAMB–1	9.8	–41.6	2.75
		ZAMB–2	10.4	–35.0	2.70
Zimbabwe	Sandawana	SAND–1	8.0	–53.3	2.30
		SAND–2	6.9	–25.0	2.80
ASIA					
Afghanistan	Shabaki	SHA–1	13.9	–45.8	2.05
	Kendjt	K1	13.6	–45.5	1.93
	Khalat–1	Khal	13.35	–45.5	2.04
	Gujari	Guj	13.25	–47.8	2.17
India	Rajhastan	96–16–1	10.8	–43.4	2.57
Pakistan	Khaltaro	KHAL–1	10.6	–67.7	2.12
	Swat Valley	Swat 1	15.4	–51	
		Swat 2	15.8	–48	
		Em1	15.1	–42	
		Em2	15.9	–32	
		Em3	15.4	–37	
		Em4	15.7	–44	
		Em5	16.2	–39	
EUROPE					
Austria	Habachtal	Hab–3	7.3	–21.1	3.33
		Hab–4	7.2	–23.0	2.92
		Hab–6	6.9	–24.4	2.95
Bulgaria	Rila	Rila 1	9.5	–30.2	1.95
		Rila 2	9.4	–29.8	2.40
		Rila 3	9.3	–32.7	2.21
Norway	Mjosa–See	NOR–1	9.4	–40.8	1.10
		NOR–2	9.6	–37.8	1.10
Russia	Malysheva	OUR–4	10.2	–40.8	2.83
		PRK–14	11.0	–40.7	2.35
Spain	Franqueira	FRAN–1	9.75	–23.3	2.30
OCEANIA					
Australia	Emmaville	EMM–II	11.2	–83.4	0.87
	Poona	POO–1	7.0	–43.8	2.49
	Menzies	MEN–1	9.0	–42.3	1.98
	Torrington	TO–1	9.9	–89.0	0.83
SYNTHETIC EMERALD (Hydrothermal)					
Russia	Tairus (1997)	TAIR–1	–2.1	–114.2	1.19
Russia	Bidulite (1997)	AM–07	–9.0	–95.4	1.53
Russia	Krasnoïarsk	KR–1	–6.3	–104.8	1.03
Australia	Biron	BIR–1	–5 0	–80.5	1.31
Russia	Bukin	BUK–1	–0.9	–109.3	1.16
U.S.A	Regency (1983)	REG–1	–1.6		

* or H_2O^+.

Geochronology

Mica for $^{40}Ar/^{39}Ar$ dating was taken from the mica-rich schist close to a quartz vein and within the zone of emerald mineralization. The results of the argon isotope study may be obtained from the authors or the Depository of Unpublished Data, CISTI, National Research Council, Ottawa, Ontario K1A 0S2, Canada. The mica yields a flat Ar–Ar age spectrum (Fig. 13) The age spectrum does not indicate the presence of an excess argon component or any diffusive loss of argon, and yields a plateau age of 108.7 ± 1.2 Ma (2σ error, calculated from 13 steps comprising 98% of the total ^{39}Ar released). The total (integrated) gas age of 107.4 ± 1.1 Ma is identical to the plateau age.

The $^{40}Ar/^{39}Ar$ age of *ca.* 109 Ma obtained for the mica is only slightly younger than U–Pb zircon ages of *ca.* 112 Ma reported for several of the felsic intrusions in the Finlayson Lake area, including the pluton immediately east of the emerald showing (Mortensen 1999). The temperatures obtained using the quartz–tourmaline geothermometer (approximately 365 and 498°C; Marshall *et al.* 2002) are higher than the closure temperature of biotite (*T* in the range 280–360°C: Harrison *et al.* 1985). However, the relationship between growth (or thermal resetting) of the mica and formation of the

TABLE 7. STABLE ISOTOPE AND FLUID INCLUSION DATA FOR NATURAL EMERALD

Country	Locality	$\delta^{18}O$ emerald (‰)	δD channel (‰)	Temperature of emerald formation (°C)	Fluid inclusions references
AMERICAS					
Brazil	Coqui^{I}	12.1	-41.3*	250-300	Cheilletz *et al.* (1991)
	Capoeirana^{I}	6.2(1)	-40.0*	450-650§	De Souza *et al.* (1992)
	Carnaíba^{I}	9.05(1)	-53.7*	300-350	Giuliani *et al.* (1997b)
	Socotó^{I}	10.9	-41.0*	300-350	Giuliani *et al.* (1997b)
	Porangatu^{I}	11.0(3)†	-40.0(5.0)†	350-630§	Barros & Kinnaird (1985) Cassedanne & Barros (1986)
	S. Terezinha^{II}	12.2(1)	-33.0(3.1)*	330-490	Giuliani *et al.* (1997b)
Canada	Regal Ridge	13.3(10)	-57.3(2.2)	260-340	This study
		14.0(7)	-59.8(2.2)	260-340	
Colombia	Eastern zone^{II}	17.4(6)	-19.1(7.7)*	260-340§	Giuliani *et al.* (1992)
	Western zone^{II}	21.1(1.9)	-20.4(5.6)*	300-320§	Cheilletz *et al.* (1994)
				325	Ottaway *et al.* (1994)
AFRICA					
Egypt	Sikait^{II}	10.4(1.0)	-59.0(3.0)	260-380	Abdalla & Mohamed (1999)
Nigeria	Kaduna^{I}	9.7(2.0)	-49.0(4.0)	400-450	Vapnik & Moroz (2000)
S. Africa	Leydsdorp^{I}	9.6(1)	-29.0(4.0)	450-500§	Nwe & Morteani (1993)
Tanzania	Sumbawanga^{I}	11.7	-41.3	380-400	Moroz & Vapnik (1999)
Zambia	Miku^{I}	10.1(3)	-38.0(3.0)	240	Moroz & Vapnik (1999)
ASIA					
Afghanistan	Panjsher^{II}	13.5(3)	-46.2(3)	200-350	Seal (1989)
				300-400§	Vapnik & Moroz (2000)
Pakistan	Khaltaro^{I}	10.65(10)	-87.7	400-550§	Laurs *et al.* (1996)
	Swat Valley^{II}	15.6(3)	-41.9(5.6)‡	380-450§	Seal (1989)
EUROPE					
Austria	Habachtal^{II}	7.1(2)	-23.0(1.0)	500-550§	Nwe & Grundmann (1990)
Bulgaria	Rila^{I}	9.4(1)	-31.0(1.0)	300-400	Alexandrov *et al.* (2001)
Russia	Malysheva^{I}	10.6(4)	-40.8(1.0)	270-280	Moroz & Vapnik (1999)
Spain	Franqueira^{I}	9.8	-23.3	320-380§	Martin-Izard *et al.* (1995)

Note: I = Type I deposit; **II** = Type 2 deposit (Schwarz & Giuliani 2001). Hydrogen-isotope composition of water from channels (δD channel) was obtained on the same samples studied for the oxygen-isotope composition of emerald ($\delta^{18}O$) and published in Giuliani *et al.* (1998). δD data references: * = Giuliani *et al.* (1997a). The δD values for the Colombian emeralds are average values (Eastern emerald zone, n = 7 deposits; western emerald zone, n = 8 deposits); † = Fallick & Barros (1987); ‡ = from Arif *et al.* (1996). Fluid-inclusions and temperature of emerald formation: § = trapping temperature; without symbols = minimum trapping temperature (range of homogenisation temperatures).

emerald crystals is unknown. The mica is part of a regional metamorphic mineral assemblage within the host schists, and the $^{40}Ar/^{39}Ar$ age therefore represents the time at which the mica last cooled through its closure temperature. The age of 109 Ma that we obtained for the mica could reflect either the age of a thermal overprint related to the event that produced the emerald crystals, or cooling following intrusion of the adjacent granitic pluton at ~112 Ma, or both.

GENETIC CLASSIFICATION

Numerous schemes of genetic classication have been proposed for emerald deposits. The two main types of deposits generally distinguished are those related to granitic intrusions (Type I of Schwarz & Giuliani 2001) and those associated with hydrothermal activity in tectonically active areas in which fluid circulation is controlled by tectonic features such as thrust faults and shear zones (Type II of Schwarz & Giuliani 2001). Most Type-I deposits are in direct contact with a granitic body or granitic pegmatite dikes. As related previously, the Colombian Type-II deposits are unique in that they resulted from the thermochemical reduction of evaporitic sulfate brines, so the Be had a sedimentary origin (Ottaway *et al.* 1994). In both types of deposits, the fluids responsible for emerald formation may be magmatic or metamorphic in origin, or may be a mixture of both. An alternative genetic model has been proposed by Grundmann & Morteani (1989), who suggested that in some deposits, growth of the emerald is a result of syn- to post-tectonic reactions under low-grade regional metamorphism.

In the Regal Ridge showing, the emerald crystals are contained in tourmaline–scheelite-bearing layers of mica schist at the margins of quartz veins. Geochemical and field evidence suggests that the emerald-bearing assemblages resulted from the circulation and infiltration of fluids that were channeled by fractures and that interacted with the Cr–V-bearing boninites. The fractures are filled by quartz, and emerald is restricted to the most proximal part of the veins. The Cr and V were most likely derived from nearby mafic and ultramafic rocks, with the specific source of Be being the nearby granite.

The Regal Ridge showing is most likely a Type-I deposit. Although the showing is not in direct contact with a granitic body or granitic pegmatite dikes, it is related to tourmaline-rich quartz veins. Although the maximum pressure suggested by the fluid-inclusion study (2.5 kbar) is within the range expected for peg-

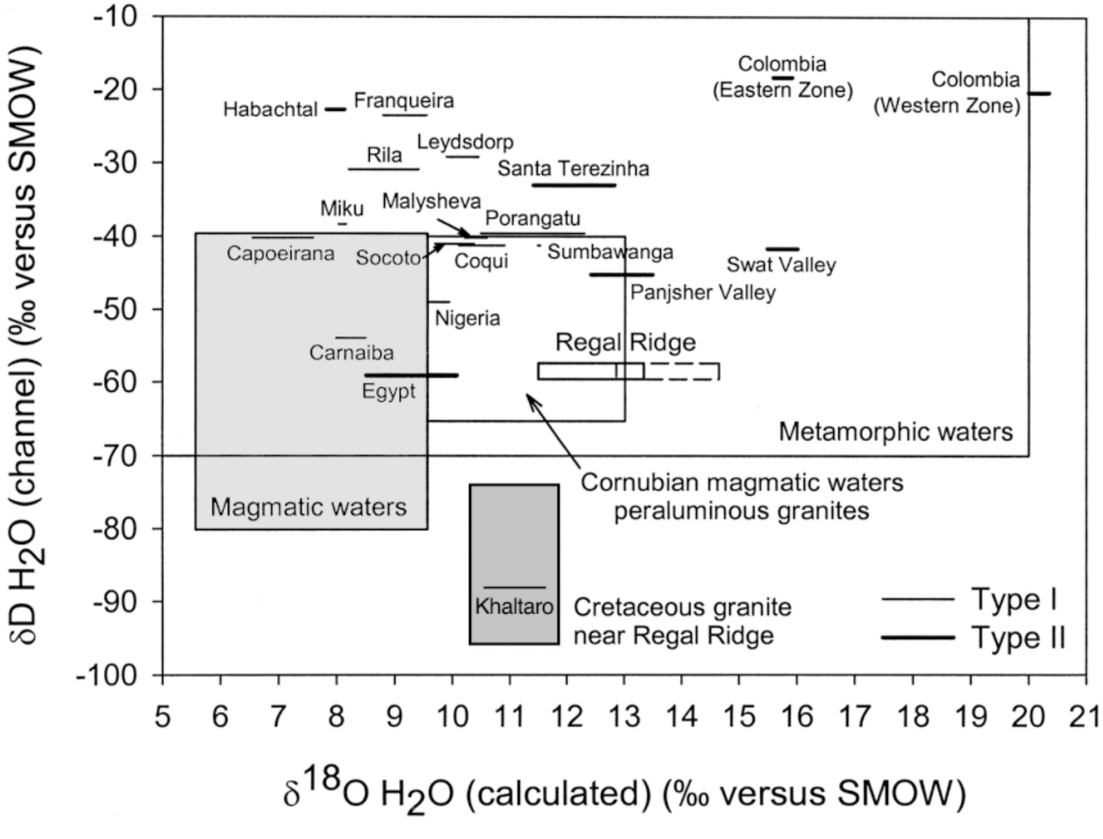

FIG. 11. Channel δD H$_2$O *versus* calculated δ^{18}O H$_2$O (‰, SMOW) for samples of Regal Ridge emerald and emerald from other deposits (data from Table 5). The isotopic compositional fields are from Sheppard (1986). The equation used to calculate oxygen fractionation between beryl and water is from Taylor *et al.* (1992): $10^3 \ln \alpha_{\text{beryl–water (250–500°C)}} = 1.579(10^6/T^2) - 0.645(10^3/T) - 2.522$, where T is temperature in Kelvin. The field for the Regal Ridge emerald samples is calculated for the temperature ranges given by both the fluid-inclusion (solid box) and quartz–tourmaline oxygen isotopic (dashed box) studies. The field for fluids in equilibrium at 500–800°C with biotite and muscovite from the Cretaceous granite near the Regal Ridge showing is shown in grey.

matite formation, the minimum pressure (1 kbar) is within the range in which mineralized quartz veins are the more common form of granite-related deposit (Ishihara & Takenouchi 1980, Strong 1988). These quartz veins may be rich in W, such as at Panasqueira (Kelly & Rye 1979). The Regal Ridge quartz veins occur in proximity to an S-type granite, exposed 1 km southeast and outcropping 600 m to the east of the Regal Ridge showing. This granite contains tourmaline-bearing quartz veins that are similar to those associated with the emerald. In addition, the presence of scheelite, emerald, tourmaline and F–Rb–Cs-rich phlogopite indicates a supply of alkali and incompatible elements such as Rb, Be, Cs, F, W and B from the fluids. Such elements are generally concentrated in S- or A-types granites. The granitic intrusion proximal to the Regal Ridge emerald deposit is Be-, F-, Li- and W-bearing, and thus is a good candidate for the source of the Be-bearing parent fluids of emerald. We note as well that the chemical composition of the parental fluids is similar to the typical H_2O–CO_2–NaCl (± CH_4) low- to medium-salinity and low-temperature fluids associated with Be–Sn–W granite-related mineralization described in the Cornubian magmatism (Alderton & Harmon 1991) and with other emerald deposits such as Franqueira (Fuertes-Fuente *et al.* 2000) and Gravellotte (Nwe & Morteani 1993). Finally, the isotopic composition of the parental H_2O lies partly within the range defined by fluids in equilibrium with S-type granites such as those from the Cornubian batholith in England (Fig. 11; Sheppard 1986).

BERYL AND EMERALD IN THE NORTHERN CANADIAN CORDILLERA

Numerous localities of beryl and one additional occurrence of emerald have been described from the Cordillera in northern Canada. In 1997, R. Berdahl discovered V-dominant emerald near the Lened tungsten showing in the southwestern Northwest Territories. The property, which is currently held by Liberty Mineral Exploration Incorporated, is underlain by a rare-element-enriched two-mica pluton and associated rare-element pegmatites, around which are developed significant amounts of W-bearing skarn (NORMIN.DB number 084048; www.inacnt.internorth.ca/scripts/default.htm). The emerald crystals are in a phlogopite schist that developed along the contact zone between a

TABLE 8. GEOCHEMISTRY OF GRANITE PROXIMAL TO THE REGAL RIDGE EMERALD SHOWING, YUKON TERRITORY

Oxide/ element	Outcrop granite	Main granite	Element	Outcrop granite	Main granite
P_2O_5 (wt.%)	0.08	0.11	Sr	64.8	170.5
SiO_2	73.93	70.9	Y	9	11.5
TiO_2	0.14	0.27	Zr	-	486
Al_2O_3	14.29	15.15	Nb	12	15
Cr_2O_3	<0.01	0.03	Mo	1	-
Fe_2O_3	0.76	1.25	Ag	<1	<1
MgO	0.26	0.33	Sn	7	47
CaO	0.76	1.33	Cs	15.3	33.2
MnO	0.03	0.03	Ba	202	529
FeO	0.6	0.74	La	30	47.5
Na_2O	3.71	3.35	Ce	58.5	111
K_2O	4.37	5.27	Pr	6.5	11.1
LOI	0.77	1.0	Nd	18.5	35.5
Total	99.7	99.8	Sm	3.8	6.3
			Eu	0.2	0.8
Li (ppm)	148	97	Gd	2.4	4.5
Be	12	13.2	Tb	0.3	0.6
B	75	42	Dy	1.7	2.4
F	630	1010	Ho	0.3	0.4
Cl	<200	-	Er	0.8	0.9
Ar	55	-	Tm	<0.1	<0.5
Sc	-	-	Yb	0.8	0.9
V	5	23	Lu	<0.1	0.1
Cr	6	-	Hf	2	11
Co	22.5	2.2	Ta	11.5	2.8
Ni	5	9	W	231	7
Cu	5	29	Tl	1.5	1
Zn	20	86	Pb	45	50
Ga	27	34	Th	17	24
Rb	405	410	U	12	6

Note: Most major elements were analyzed using XRF, and most trace elements by ICP-MS or ICP-ES. Li, Be, Cr, Mo were determined by AAS; B and Cl by INAA; FeO by titration.

TABLE 9. GEOCHEMISTRY OF SCHIST, REGAL RIDGE EMERALD SHOWING, YUKON TERRITORY

Oxide/ element	Schist 1	Schist 2	Element	Schist 1	Schist 2
P_2O_5 (wt %)	0.04	0.03	Rb	5.6	105
SiO_2	59.2	56.1	Sr	71	46.4
TiO_2	0.17	0.24	Y	5.9	6.5
Al_2O_3	11.3	10.35	Zr	11.0	132.5
Cr_2O_3	-	0.09	Nb	0.68	1
Fe_2O_3	1.5	1.93	Mo	-	-
MgO	8.88	11.5	Ag	-	<1
CaO	6.61	7.59	Sn	-	11
MnO	0.1	0.16	Cs	10.00	72.2
FeO	4.5	6.7	Ba	130	183.5
Na_2O	2.0	1.43	La	1.00	2.2
K_2O	0.13	0.83	Ce	1.90	1.1
H_2O	3.6	-	Pr	0.24	0.1
CO_2	2.7	-	Nd	1.10	0.7
LOI	-	2.32	Sm	0.39	0.4
Total	100.73	99.27	Eu	0.10	0.1
			Gd	0.65	0.6
Li (ppm)	-	84	Tb	0.12	0.1
Be	-	1.1	Dy	0.92	1.1
B	-	<5	Ho	0.20	0.2
F	-	190	Er	0.62	0.7
Cl	-	-	Tm	0.10	<0.5
Ar	-	-	Yb	0.70	0.7
Sc	30	-	Lu	0.13	0.1
V	136	190	Hf	0.34	2
Cr	520	-	Ta	0.05	<0.5
Co	34	41.2	W	-	2
Ni	155	126	Tl	-	1
Cu	111	27	Pb	1	<5
Zn	53	82	Th	0.12	<1
Ga	7.8	8	U	0.12	<0.5

Note: Most major elements were analyzed using XRF, and most trace elements by ICP-MS or ICP-ES. Li, Be, Cr, Mo were determined by AAS; B and Cl by INAA; CO_2 and H_2O by infrared spectroscopy; F by specific ion potentiometry; FeO by titration..

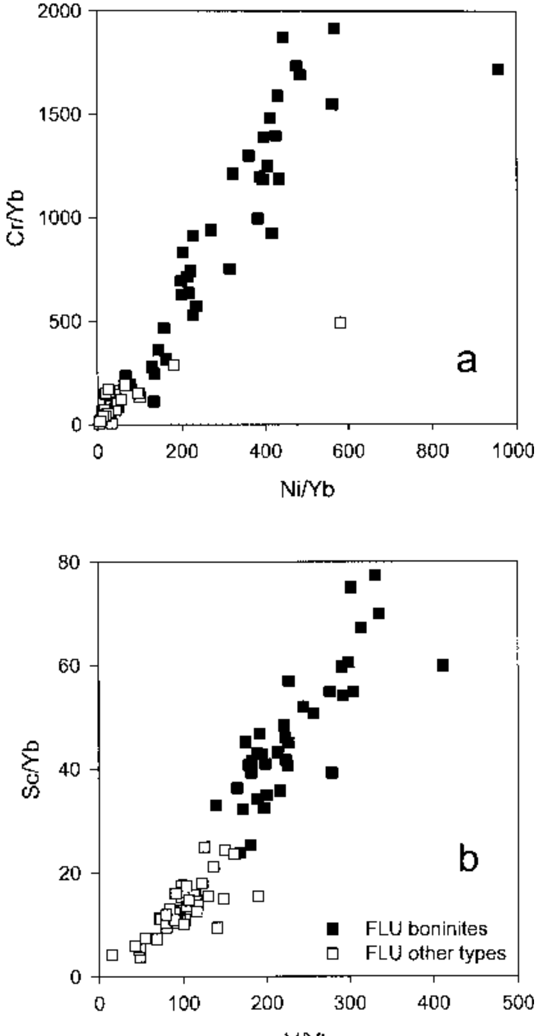

FIG. 12. (a) Cr/Yb – Ni/Yb and (b) Sc/Yb – V/Yb plots illustrating the high transition-metal contents of the Fire Lake boninites in relation to other mafic rocks of the Fire Lake unit. These boninitic mafic rocks are spatially proximal to the Regal Ridge showing. Data are from Piercey *et al.* (2001).

rare-element pegmatite and Devonian–Mississippian black shales. The latter are enriched in platinum-group elements, V, and Cr (W. Goodfellow, pers. commun.). The crystals are transparent to translucent and up to 2.0 cm in length. The Lened showing is not far from the O'Grady batholith, site of the Stargazer gem tourmaline (elbaite) property, discovered in 1995 (Groat *et al.* 1995a, b, Groat & Ercit 1996, Ercit *et al.* 1998).

A review of assessment reports (Yukon and British Columbia MINFILE; www.em.gov.bc.ca/Mining/Geolsurv/Minfile/default.htm) shows numerous Be and beryl occurrences in southern Yukon and northern British Columbia. Analyses of a scapolite skarn with scheelite at the Myda claim (Yukon MINFILE 105G/071), approximately 20 km south of the Regal Ridge showing, show 0.05 to 0.09 wt.% BeO, considered to be present in vesuvianite. Beryl has been reported from the Logtung W–Mo deposit (Yukon MINFILE 105B/039), the JC (Viola) Sn-bearing skarn claims (Yukon MINFILE 105B/040), and the Ice Lakes area (Groat *et al.* 1995a), all just north of the British Columbia – Yukon border. Beryl also has been reported from the following showings and prospects in northern British Columbia (listed west to east): Jennings River (British Columbia MINFILE 104O/028), Ash Mountain (104O/021), Blue Light (104O/005), Gazoo (104O/045), Low Grade (104P/026), Haskins Mountain (104P/020) and Cassiar Beryl (104P/024). Most of these are associated with Cretaceous granitic plutons, in particular the Cassiar batholith. The occurrences listed here (including the Regal Ridge showing) define a Be-rich area approximately 265 (NW–SE) by 125 km (NE–SW) that straddles the British Columbia – Yukon border and the Tintina Fault. Another area with obvious potential for Be mineralization is the offset part of the Yukon – Tanana Terrane southwest of the Tintina Fault, close to Dawson City.

The Regal Ridge emerald showing is one of a number of significant gem deposits discovered in northern Canada in the last decade, the most notable of which are the occurrences of diamond in the Northwest Territories. A small number of gems have already been fashioned from the Regal Ridge material (Fig. 14). It is still too soon to tell if the Regal Ridge showing will become an emerald producer; additional work (including bulk sampling) must be completed before the economic potential of the deposit can be assessed.

ACKNOWLEDGEMENTS

The authors thank B.C. Pemberton for preparation of the electron-microprobe mounts and for help with the SEM study, K.E. Parker for editing the manuscript, and Dr. F. Notary (GemTechLab, Geneva) for providing samples of synthetic emerald for the stable isotopic study. The manuscript was improved by comments from F.J. Wicks, an anonymous reviewer, B.S. Wilson, and R.F. Martin. Financial support was provided by the Natural Sciences and Engineering Research Council of Canada in the form of Research Grants to LAG and DDM, and by the Canadian Museum of Nature in the form of a Research Advisory Committee grant to TSE. This paper is dedicated to the memory of M.T. Green (1984–2001), who participated in its preparation.

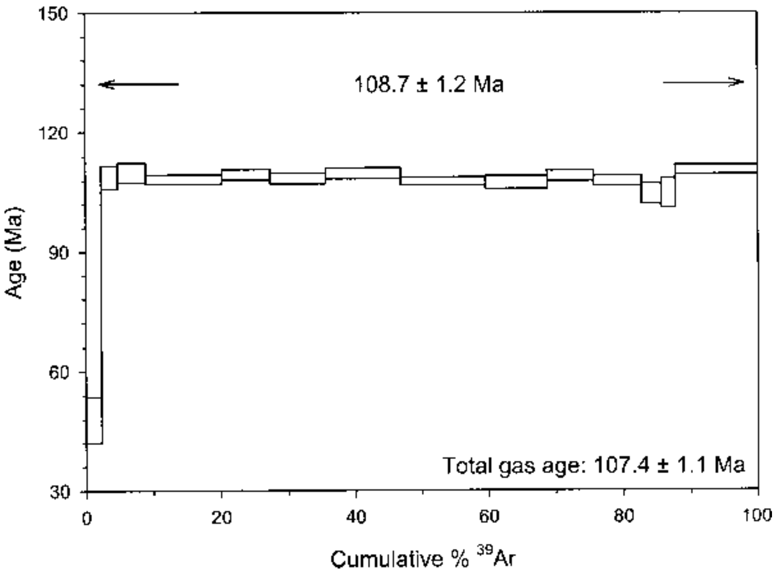

FIG. 13. Cumulative proportion of ^{39}Ar *versus* age (Ma) for a mica sample from the schist close to the emerald mineralization.

REFERENCES

ABDALLA, H.M. & MOHAMED, F.H. (1999): Mineralogical and geochemical investigation of emerald and beryl mineralisation, Pan-African Belt of Egypt: genetic and exploration aspects. *J. Afr. Earth Sci.* **28**, 581-598.

AINES, R.D. & ROSSMAN, G.R. (1984): The high-temperature behavior of water and carbon dioxide in cordierite and beryl. *Am. Mineral.* **69**, 319-327.

ALDERTON, D.H.M. & HARMON, R.S. (1991): Fluid inclusion and stable-isotope evidence for the origin of mineralizing fluids in southwest England. *Mineral. Mag.* **55**, 605-611.

ALEXANDROV, P., GIULIANI, G. & ZIMMERMANN, J.-L. (2001): Mineralogy, age and fluid geochemistry of the Rila emerald deposit, Bulgaria. *Econ. Geol.* **96**, 1469-1476.

ARIF, M., FALLICK, A.E. & MOON, C.J. (1996): The genesis of emeralds and their host rocks from Swat, northwestern Pakistan: a stable-isotope investigation. *Mineral. Deposita* **31**, 255-268.

AURISICCHIO, C., FIORAVANTI, G., GRUBESSI, O. & ZANAZZI, P.F. (1988): Reappraisal of the crystal chemistry of beryl. *Am. Mineral.* **73**, 826-837.

BAKKER, R.J. (1999): Adaptation of the Bowers and Helgeson (1983) equation of state to the H_2O–CO_2–CH_4–N_2–NaCl system. *Chem. Geol.* **154**, 225-236.

________ & DIAMOND, L.W. (2000): Determination of the composition and molar volume of H_2O–CO_2 fluid inclusions by microthermometry. *Geochim. Cosmochim. Acta* **64**, 1753-1764.

BANKS, D.A., GIULIANI, G., YARDLEY, B.W.D. & CHEILLETZ, A. (2000): Emerald mineralization in Colombia: fluid chemistry and the role of brine mixing. *Mineral. Deposita* **35**, 699-713.

BARROS, J.C. & KINNAIRD, J.A. (1985): Fluid inclusion studies of emeralds and green beryls from the Porangatu deposit, Goiás state, Brazil. *European Current Research on Fluid Inclusions Meeting* (*ECROFI VIII*), *Abstr.*

BEUS, A.A. (1966): *Geochemistry of Beryllium and Genetic Types of Beryllium Deposits*. Freeman, New York, N.Y.

________ & MINEEV, D.A. (1972): Some geological and geochemical features of the emerald-bearing Muzo–Coscuez emerald zone, Cordillera Oriental, Colombia. *Geol. Rudn. Mestorozhd.* **16**, 18-30.

BLOSS, F.D. (1981): *The Spindle Stage: Principles and Practice*. Cambridge University Press, Cambridge, U.K.

BOTTINGA, Y. & JAVOY, M. (1973): Comments on oxygen isotope geothermometry. *Earth Planet. Sci. Lett.* **20**, 250-265.

________ & ________ (1975): Oxygen isotope partitioning among the minerals in igneous and metamorphic rocks. *Rev. Geophys. Space Phys.* **13**, 401-418.

FIG. 14. (left) A faceted gemstone from the Regal Ridge showing. The gem weighs 0.11 ct and is 2.9 by 2.7 mm in size. (right) A cabochon from the Regal Ridge occurrence. The cabochon weighs 2.10 ct and measures 15.1 by 6.9 mm (photographs courtesy of B.S. Wilson of Alpine Gems Inc.).

BROWN, G.E., JR. & MILLS, B.A. (1986): High-temperature structure and crystal chemistry of hydrous alkali-rich beryl from the Harding pegmatite, Taos County, New Mexico. *Am. Mineral.* **71**, 547-556.

CASSEDANNE, J.P. & BARROS, J.C. (1986): Some emerald deposits in Goias. *Revue de Gemmologie A.F.G.* **88**, 9-12.

CHEILLETZ, A., FERAUD, G., GIULIANI, G. & RODRIGUEZ, C.T. (1991): ^{40}Ar/ ^{39}Ar laser-probe dating of the Colombian emerald deposits: metallogenic implications. *In* Source, Transport and Deposition of Metals. (M. Pagel & Leroy, J.L., eds.). A. A. Balkema. Rotterdam, Netherlands (373-376).

________, _______, _______ & ________ (1994): Time–pressure and temperature constraints on the formation of Colombian emeralds; an ^{40}Ar/ ^{39}Ar laser microprobe and fluid inclusion study. *Econ. Geol.* **89**, 361-380.

CRAWFORD, A.J., FALLOON, T.J. & GREEN, D.H. (1989): Classification, petrogenesis, and tectonic setting of boninites. *In* Boninites and Related Rocks (A.J. Crawford, ed.). Unwin Hyman, London, U.K. (1-49).

DE SOUZA, J.L., MENDES, J.C., DA SILVEIRA BELLO, R.M., SVISERO, D.P. & VALARELLI, J.V. (1992): Petrographic and microthermometrical studies of emeralds in the "Garimpo" of Capoeirana, Nova Era, Minas Gerais State, Brazil. *Mineral. Deposita* **27**, 161-168.

DIAMOND, L.W. (1992): Gas clathrate hydrates in fluid inclusions: phase equilibria and applications. *Fourth Biennial Pan-American Conference on Research on Fluid Inclusions* (*PACROFI IV*), *Program Abstr.*, 119-122.

________ (2001): Review of the systematics of CO_2–H_2O fluid inclusions. *Lithos* **55**, 69-99.

ERCIT, T.S., GROAT, L.A. & GAULT, R.A. (1998): A gem tourmaline-bearing aplite–pegmatite complex, O'Grady batholith, western NWT. *Dep. Indian Affairs and Northern Development, Econ. Geol. Ser.* **1998–9**.

FALLICK, A.E. & BARROS, J.G. (1987): A stable-isotope investigation into the origin of beryl and emerald from the Porangatu deposits, Goiás state, Brazil. *Chem. Geol., Isotope Geosci.* **66**, 293-300.

FUERTES-FUENTE, M., MARTIN-IZARD, A., BOIRON, M.C. & VIÑUELA, J.M. (2000): P–T path and fluid evolution in the Franqueira granitic pegmatite, central Galicia, northwestern Spain. *Can. Mineral.* **38**, 1163-1175.

GEHRIG, M. (1980): *Phasengleichgewichte und PVT-Daten ternärer Mischungen aus Wasser, Kohlendioxid und Natriumchlorid bis 3 kbar und 550°C.* Ph.D. thesis, University of Karlsruhe University, HochschulVerlag, Freiburg, Germany.

GIULIANI, G., CHEILLETZ, A., ARBOLEDA, C., CARRILLO, V., RUEDA, F. & BAKER, J.H. (1995): An evaporitic origin of the parent brines of Colombian emeralds: fluid inclusion and sulphur isotope evidence. *Eur. J. Mineral.* **7**, 151-165.

________, ________, ZIMMERMANN, J.-L., RIBEIRO-ALTHOFF, A.M., FRANCE-LANORD, C. & FERAUD, G. (1997a): Les gisements d'émeraude du Brésil: genèse et typologie. *Chronique de la Recherche Minière* **526**, 17-61.

________, France-Lanord, C., Coget, P., Schwarz, D., Cheilletz, A., Branquet, Y., Giard, D., Martin-Izard, A., Alexandrov, P. & Piat, D.H. (1998): Oxygen isotope systematics of emerald: relevance for its origin and geological significance. *Mineral. Deposita* **33**, 513-519.

________, ________, Zimmermann, J.-L., Cheilletz, A., Arboleda, C., Charoy, B., Coget, P., Fontan, F. & Giard, D. (1997b): Fluid composition, δD of channel H_2O, and $\delta^{18}O$ of lattice oxygen in beryls: genetic implications for Brazilian, Colombian, and Afghanistani emerald deposits. *Int. Geol. Rev.* **39**, 400-424.

________, Sheppard, S.M.F., Cheilletz, A. & Rodriguez, C. (1992): Contribution de l'étude des phases fluides et de la géochimie isotopique $^{18}O/^{16}O$, $^{13}C/^{12}C$ à la genèse des gisements d'émeraude de la Cordillère orientale de la Colombie. *C.R. Acad. Sci. Paris* **314**, *Sér.* II, 269-274.

Goldschmidt, V.M. (1954): *Geochemistry.* Clarendon Press, Oxford, U.K.

Graziani, G., Gübelin, E. & Lucchesi, S. (1983): The genesis of an emerald from the Kitwe District, Zambia. *Neues Jahrb. Mineral., Monatsh.*, 175-186.

Groat, L.A. & Ercit, T.S. (1996): Granitic pegmatites of mixed NYF–LCT affinity from the O'Grady batholith, western Northwest Territories. *Dep. of Indian Affairs and Northern Development, Econ. Geol. Ser.* **1996-7**.

________, ________, Mortensen, J.K. & Mauthner, M.H.F. (1995a): Granitic pegmatites in the Canadian Cordillera: Yukon and Northwest Territories. *Exploration and Geological Services Division, Indian and Northern Affairs, Canada, Open File* **1995-14**.

________, ________, ________ & ________ (1995b): Granitic pegmatites in the western Northwest Territories. *Dep. of Indian Affairs and Northern Development, Econ. Geol. Ser.* **1995-10**.

Grundmann, G. & Morteani, G. (1989): Emerald mineralisation during regional metamorphism: the Habachtal (Austria) and Leydsdorp (Transvaal, South Africa) deposits. *Econ. Geol.* **84**, 1835-1849.

Gübelin, E.J. (1958): Emeralds from Sandawana. *J. Gemmology* **6**, 340-354.

________ (1989): Gemological characteristics of Pakistan emeralds. *In* Emeralds of Pakistan: Geology, Gemology and Genesis (A.H. Kazmi & L.W. Snee, eds.). Van Nostrand Reinhold Company, New York, N.Y. (75-91).

Hammarstrom, J.M. (1989): Mineral chemistry of emeralds and some associated minerals from Pakistan and Afghanistan: an electron microprobe study. *In* Emeralds of Pakistan: Geology, Gemology and Genesis (A.H. Kazmi & L.W. Snee, eds.). Van Nostrand Reinhold Company, New York, N.Y. (125-150).

Hanni, H.A. & Klein, H.H. (1982): Ein Smaragdvorkommen in Madagaskar. *Z. Deutsch. Gemmol. Gesellsch.* **21**, 71-77.

Harrison, T.M., Duncan, I. & McDougall, I. (1985): Diffusion of ^{40}Ar in biotite: temperature, pressure and compositional effects. *Geochim. Cosmochim. Acta* **49**, 2461-2468.

Hickman, A.C.J. (1972): The Miku emerald deposit. *Geol. Surv. Zambia, Econ. Rep.* **27**.

Ishihara, S. & Takenouchi, S. (1980): Granitic magmatism and related mineralization. *Mining Geol.* **8**, 1-247.

Kelly, W.C. & Rye, R.O. (1979): Geologic, fluid inclusion, and stable isotope studies of the tin–tungsten deposits of Panasqueira, Portugal. *Econ. Geol.* **74**, 1721-1822.

Kotzer, T.G., Kyser, T.K., King, R.W. & Kerrich, R. (1993): An empirical oxygen- and hydrogen-isotope geothermometer for quartz–tourmaline and tourmaline–water. *Geochim. Cosmochim. Acta* **57**, 3421-3426.

Kovaloff, P. (1928): Geologist's report on Somerset emeralds. *S. Afr. Mining Engineer. J.* **39**, 101-103.

Kozlowski, A., Metz, P. & Estrada Jaramillo, H.A.E. (1988): Emeralds from Somondoco, Colombia: chemical composition, fluid inclusions and origin. *Neues Jahrb. Mineral., Abh.* **159**, 23-49.

Laurs, B.M., Dilles J.H. & Snee L.W. (1996): Emerald mineralization and metasomatism of amphibolite, Khaltaro granitic pegmatite hydrothermal vein system, Haramosh Mountains, northern Pakistan. *Can. Mineral.* **34**, 1253-1286.

Lawrence, R.D., Kazmi, A.H. & Snee, L.W. (1989): Geological setting of the emerald deposits. *In* Emeralds of Pakistan: Geology, Gemology and Genesis (A.H. Kazmi & L.W. Snee, eds.). Van Nostrand Reinhold Company, New York, N.Y. (13-38).

Leitmeier, H. (1937): Das Smaragdvorkommen in Habachtal in Salzburg und seine Mineralien. *Tschermaks Mineral. Petrogr. Mitt.* **49**, 245-368.

Marshall, D.D., Groat, L.A., Giuliani, G., Murphy, D.C., Mattey, D., Ercit, T.S., Wise, M.A., Wengzynowski, W. & Eaton, W.D. (2002): Pressure, temperature, and fluid conditions during emerald precipitation, southeastern Yukon: fluid inclusion and stable isotope evidence. *Chem. Geol.* **186** (in press).

Martin, H.J. (1962): Some observations on southern Rhodesian emeralds and chrysoberyls. *J. Chamber of Mines* **4**, 34-38.

Martin-Izard, A., Paniagua, A., Moreiras, D., Acevedo, R.D., Marcos-Pascual, C. (1995): Metasomatism at a granitic pegmatite–dunite contact in Galicia; the Franqueira occurrence of chrysoberyl (alexandrite), emerald, and phenakite. *Can. Mineral.* **33**, 775-792.

MCDOUGALL, I. & HARRISON, T.M. (1988): *Geochronology and Thermochronology by the $^{40}Ar/^{39}Ar$ method.* Oxford University Press, Oxford, U.K.

MOROZ, I. & VAPNIK, YE. (1999): Fluid inclusions in emeralds from schist-type deposits. *Can. Gemmologist* **20**, 8-14.

________ & ________ (2001): Fluid inclusions in Panjshir emerald (Afghanistan). *European Current Research on Fluid Inclusions Meeting* (*ECROFI XVI*), *Abstr.*

MORTENSEN, J.K. (1992): Pre-Mid-Mesozoic tectonic evolution of the Yukon–Tanana Terrane, Yukon and Alaska. *Tectonics* **11**, 836-853.

________ (1999): YUKONAGE, an isotopic age database for the Yukon Territory. *In* Yukon Digital Geology (S.P. Gordey & A.J. Makepeace, eds.). *Geol. Surv. Can., Open File* **D3826**; *Exploration and Geological Services Division, Yukon, Indian and Northern Affairs Canada, Open File* **1999-1**(**D**).

________, HART, C.J.R., MURPHY, D.C. & HEFFERNAN, S. (2000): Temporal evolution of early and mid-Cretaceous magmatism in the Tintina Gold Belt. *In* The Tintina Gold Belt: Concepts, Exploration and Discoveries (J.L. Jambor, ed.). *British Columbia and Yukon Chamber of Mines, Spec. Vol.* **2**, 49-57.

________ & JILSON, G.A. (1985): Evolution of the Yukon–Tanana Terrane: evidence from southeastern Yukon Territory. *Geology* **13**, 806-810.

MURPHY, D.C. (1997): Preliminary geological map of Grass Lakes area, Pelly Mountains, southeastern Yukon (105G/7). *Exploration and Geological Services Division, Indian and Northern Affairs Canada, Open File* **1997-3** (1:50,000 scale).

________ (1998a): Mafic and ultramafic meta-plutonic rocks south of Finlayson Lake, Yukon: setting and implications for the early geological and metallogenic evolution of Yukon–Tanana Terrane. *In* Cordillera Revisited: Recent Developments in Cordilleran Geology, Tectonics and Mineral Deposits (P. Mustard & S. Gareau, eds.). *Geol. Assoc. Can., Cordilleran Section Short Course, Extended Abstr.* (102-109).

________ (1998b): Stratigraphic framework for syngenetic mineral occurrences, Yukon–Tanana Terrane south of Finlayson Lake: a progress report. *In* Yukon Exploration and Geology 1997. *Exploration and Geological Services Division, Yukon, Indian and Northern Affairs Canada* (51-58).

________ & PIERCEY, S.J. (1998): Preliminary geological map of northern Wolverine Lake map area (NTS 105G/8, north half), Yukon. *Exploration and Geological Services Division, Indian and Northern Affairs Canada, Open File* **1998-4**.

________ & ________ (2000): Syn-mineralization faults and their re-activation, Finlayson Lake massive sulphide district, Yukon–Tanana Terrane, southeastern Yukon. *In* Yukon Exploration and Geology 1999 (D.S. Emond & L.H. Weston, eds.). *Exploration and Geological Services Division, Yukon, Indian and Northern Affairs Canada* (55-66).

NWE, Y.Y. & GRUNDMANN, G. (1990): Evolution of metamorphic fluids in shear zones: the record from the emeralds of Habachtal, Tauern window, Austria. *Lithos* **25**, 281-304.

________ & MORTEANI, G. (1993): Fluid evolution in the H_2O–CH_4–CO_2–NaCl system during emerald mineralization at Gravelotte, Murchinson greenstone belt, northeast Transvaal, South Africa. *Geochim. Cosmochim. Acta* **57**, 89-103.

OTERO MUÑOZ, G. & BARRIGA VILLALBA, A.M. (1948): *Esmeraldas de Colombia.* Banco de la Republica, Bogota, Colombia.

OTTAWAY, T.L. (1991): *The Geochemistry of the Muzo Emerald Deposit, Colombia.* M.Sc. thesis, Univ. Toronto, Toronto, Ontario.

________, WICKS, F.J., BRYNDZIA, L.T., KYSER, T.K. & SPOONER, E.T.C. (1994): Formation of the Muzo hydrothermal emerald deposit in Colombia. *Nature* **369**, 552-554.

PETRUSENKO, S., ARNAUDOV, V. & KOSTOV, I. (1966): Emerald pegmatite from the Urdini Lakes, Rila Mountains. *Annuaire de l'Université de Sofia, Faculté de Géologie et Géographie* **59**, 247-268 (in Bulg.).

PIERCEY, S.J. (2001): *Petrology and Tectonic Setting of Mafic and Felsic Volcanic and Intrusive Rocks in the Finlayson Lake Volcanic-Hosted Massive Sulphide* (*VHMS*) *District, Yukon, Canada: A Record of Mid-Paleozoic Arc and Back-Arc Magmatism and Metallogeny.* Ph.D. thesis, Univ. of British Columbia, Vancouver, British Columbia.

________, HUNT, J.A. & MURPHY, D.C. (1999): Lithogeochemistry of meta-volcanic rocks from Yukon–Tanana Terrane, Finlayson Lake region: preliminary results. *In* Yukon Exploration and Geology 1998 (C.F. Roots & D.S. Emond, eds.). *Exploration and Geological Services Division, Yukon, Indian and Northern Affairs Canada* (55-66).

________, MURPHY, D.C. & MORTENSEN, J.K. (2000b): Magmatic diversity in a pericratonic realm: tales from the Yukon–Tanana Terrane in the Finlayson Lake region, southeastern Yukon, Canada. *Geol. Soc. Am. Program Abstr.* **32**, A62.

________, ________, ________ & PARADIS, S.A. (2000a): Arc-rifting and ensialic back-arc basin magmatism in the northern Canadian Cordillera: evidence from the Yukon–Tanana Terrane, Finlayson Lake region, Yukon. *In* Slave – Northern Cordilleran Lithospheric Experiment (SNORCLE). *Lithoprobe Rep.* **72**, 129-138.

________, ________, ________ & ________ (2001): Boninitic magmatism in an continental margin, Yukon–Tanana terrane, southeastern Yukon, Canada. *Geology* **29**, 731-734.

RENDERS, P.J. & ANDERSON, G.M. (1987): Solubility of kaolinite and beryl to 573 K. *Appl. Geochem.* **2**, 193-203.

ROEDDER, E. (1984): Fluid inclusions. *Rev. Mineral.* **12**.

RUDOWSKI, L., GIULIANI, G. & SABATE, P. (1987): Emerald-bearing phlogopites in the proximity of the Campo Formoso and Carnaiba granites (Bahia, Brazil); an example of Proterozoic beryllium, molybdenum, and tungsten mineralization in metasomatic ultramafics. *C.R. Acad. Sci. Paris* **304**, *Sér.* II, 1129-1134.

SABOT, B., CHEILLETZ, A., DE DONATO, P., BANKS, D., LEVRESSE, G. & BARRES, O. (2001): The Panjshir–Afghanistan emerald deposit – new field and geochemical evidence for Colombian style mineralisation. *European Union of Geosciences Conf.* (*EUG XI*), *Abstr.*, 548.

SCHWARZ, D. & GIULIANI, G. (2001): Emerald deposits – a review. *Aust. Gemmol.* **21**, 17-23.

SEAL, R.S. (1989): A reconnaissance study of the fluid inclusion geochemistry of the emerald deposits of Pakistan and Afghanistan. *In* Emeralds of Pakistan: Geology, Gemology and Genesis (A.H. Kazmi & L.W. Snee, eds.). Van Nostrand Reinhold Company, New York, N.Y. (151-164).

SHEPPARD, S.M.F. (1986): Characterisation and isotopic variations in natural waters. *In* Stable Isotopes in High Temperature Geological Processes (J.W. Valley, H.P. Taylor, Jr. & J.R. O'Neil, eds.). *Rev. Mineral.* **16**, 165-183.

STEIGER, R. & JÄGER, E. (1977): Subcommission on geochronology: convention on the use of decay constants in geo- and cosmochronology. *Earth Planet. Sci. Lett.* **36**, 359-362.

STRONG, D.F. (1988): A review and model for granite-related mineral deposits. *In* Recent Advances in the Geology of Granite-Related Mineral Deposits (R.P. Taylor & D.F. Strong, eds.). *Can. Inst. Mining Metall., Spec. Vol.* **39**, 424-445.

SUZUOKI, T. & EPSTEIN, S. (1976): Hydrogen isotope fractionation between OH-bearing minerals and water. *Geochim. Cosmochim. Acta* **40**, 1229-1240.

TAYLOR, R.P., FALLICK, A.E. & BREAKS, F.W. (1992): Volatile evolution in Archean rare-element granitic pegmatites: evidence from the hydrogen-isotopic composition of channel H_2O in beryl. *Can. Mineral.* **30**, 877-893.

VAPNIK, Y. & MOROZ, I. (2000): Fluid inclusions in emerald from the Jos complex (central Nigeria). *Schweiz. Mineral. Petrogr. Mitt.* **80**, 117-129.

VLASOV, K.A. & KUTAKOVA, E.I. (1960): *Izumrudnye Kopi.* Akad. Nauk SSSR, Moscow, Russia.

WEDEPOHL, K.H. (1978): *Handbook of Geochemistry.* Springer-Verlag, Berlin, Germany.

ZAMBONINI, F. & CAGLIOTO, V. (1928): Ricerche chimiche sulla rosterite di San Piero in Campo (Isola d'Elba) e sui berilli in generale. *Gazz. Chim. Ital.* **58**, 131-152.

Received September 1, 2001, revised manuscript accepted June 6, 2002.

APPENDIX: ANALYTICAL PROCEDURES

The Philips XL30 scanning electron microscope (SEM) at the University of British Columbia, which is equipped with an energy-dispersion X-ray spectrometer (EDS), was used for preliminary examination of the electron-microprobe mounts. A JEOL 733 electron microprobe with Tracor Northern 5500 and 5600 automation, located at the Canadian Museum of Nature, was used for analysis (wavelength-dispersion mode). Operating conditions were as follows: voltage 15 kV, beam current 20 nA, and beam diameter 30 μm for emerald and 20 μm for tourmaline and phlogopite. Data for standards were collected for 50 s or to 0.25% precision (4σ level), whichever was attained first; data for samples were collected for 25 s or 200 s (for Sc, V, Cr, Mg, and Cs in emerald and for V, Cr, Rb, Sr, Cs, and Ba in phlogopite, respectively) or to 0.5% precision. An element was considered as observed only if its level of concentration was significant at the 4σ (measured) level. For analyses of emerald, the following standards were used: albite (Na, Si), almandine (Mg, Al, Fe), sanidine (K), diopside (Ca), REE glass (Sc), VP_2O_7 (V), synthetic nichromite (Cr), synthetic tephroite (Mn), and pollucite (Cs). *K*α lines were used except for Cs (*L*α); Ti was sought but not detected. For the analyses of tourmaline, the standards were synthetic phlogopite (F), sodic amphibole (Na), enstatite (Mg), anorthite (Al, Si), rubidian microcline (K), synthetic gehlenite (Ca), rutile (Ti), synthetic nichromite (Cr), synthetic tephroite (Mn), and almandine (Fe). *K*α lines were used throughout. Scandium, V, and Sn were sought but not detected. For analyses of phlogopite, the standards were synthetic phlogopite (F, Al, Si, K), albite (Na), chlorite (Mg), rubidian microcline (Rb), rutile (Ti), VP_2O_7 (V), chlorite (Cr, Fe), synthetic tephroite (Mn), pollucite (Cs), and sanbornite (Ba). *L*α lines were used for Rb, Cs, and Ba, and *K*α lines were used for all other elements. Ca, Zn, and Sr were sought but not detected. Data reduction in all cases was done with a PAP routine in XMAQNT

(C. Davidson, CSIRO, pers. commun.). Scandium, V, Cr, and Cs values for emerald were reported as both oxide wt.% and ppm.

Cell-dimension data were obtained at UBC with a Siemens *P*4 automated 4-circle diffractometer equipped with a Mo-target X-ray tube (operated at 50 kV, 35 mA) and a graphite-crystal monochrometer mounted with equatorial geometry. Fifty reflections were centered using automated search routines, and the correct unit-cell was selected from an array of real-space vectors corresponding to potential unit-cell axes. Least-squares refinement of these reflections produced the cell dimensions. Optical data were collected at UBC with a Supper spindle stage mounted on a polarizing microscope with a sodium (489 nm) filter, following the method of Bloss (1981). Index of refraction oils were calibrated with an Abbé refractometer. Densities were determined at UBC by suspension in heavy liquids consisting of bromoform diluted with acetone. After stable suspension was achieved, the liquid was transferred to a burette, and measured volumes of liquid were released into an Erlenmeyer flask. The cumulative weights and volumes were recorded; in general, at least six readings were averaged after discarding the single highest and single lowest of the resultant values that were obtained for the measured density.

Powder-diffraction data were collected at UBC with a Siemens D5000 diffractometer equipped with a diffracted-beam graphite monochromator and a Cu X-ray tube operated at 40 kV and 40 mA. Data were collected from 3 to 60° 2θ with a scanning step of 0.02° 2θ.

Fluid-inclusion microthermometric measurements were made at Simon Fraser University on doubly polished mineral chips. Phase changes within these samples were observed using a modified Linkam THMSG–600 heating–freezing stage fitted to an Olympus BX50 microscope. The stage was calibrated with two synthetic fluid-inclusions composed of pure CO_2 and H_2O at –56.6, 0.0 and 374.1°C. The stage was periodically checked against the standards. The error was invariably within 0.1°C of the two low-temperature calibration points and within 1.0°C of the higher-temperature standard. Further details are given in Marshall *et al.* (2002).

Stable-isotope data for the emerald crystals were collected at CRPG/CNRS in Vandoeuvre (France) according to the procedure of Giuliani *et al.* (1997a). The crystals were first heated to 500°C to ensure decrepitation of the fluid inclusions. The extraction of channel H_2O was carried out by dehydrating the crystals in a vacuum with a methane–oxygen flame. D/H ratios were determined using a VG 602 D mass spectrometer and are reported relative to Standard Mean Ocean Water (SMOW) using conventional notation, where δ is the relative difference in isotopic ratio between a sample and the standard, expressed in per mil (‰). The 1σ analytical precision is ±2.0‰ for δD. Oxygen isotopic ratios ($^{18}O/^{16}O$) for the emerald crystals were determined using a Cameca 1270 ion probe with a Cs^+ primary beam and electron bombardment. Analyses of the ^{16}O and ^{18}O secondary ions were done in multicollection mode, at a mass resolution of 4500. The instrumental mass-fractionation was calibrated with a set of three standards of different compositions. The $^{18}O/^{16}O$ ratios were determined with a precision of 0.4‰ (1σ). Hydrogen and oxygen isotope data for primary igneous quartz, biotite, and muscovite from the granite and for coexisting quartz and tourmaline from the quartz veins associated with the emerald mineralization were obtained at Queen's University. H_2O was removed from the sample using a 5 kW radio-frequency generator. A bromine pentafluoride extraction line was used for the oxygen, and depleted uranium was used for hydrogen. The proportion of isotopes was measured with a Finnigan Mat 252 mass spectrometer.

Whole-rock analyses of the granite and vein quartz were done by ALS Chemex Limited of North Vancouver. Lithium, Be, Cr, and Mo concentrations were determined by atomic absorption spectroscopy, B and Cl by neutron activation analysis, and F by specific ion potentiometry. The concentration of all other elements were measured by induction-coupled plasma – mass spectrometry (ICP–MS) or X-ray fluorescence (XRF). Whole-rock data for the schists and boninites were supplied by the Geological Survey of Canada in Ottawa. Concentrations of most major elements were established by XRF; the amount of FeO was determined by wet-chemical methods, and that of CO_2 and H_2O, by infrared spectroscopy. Trace-element data were obtained by ICP–ES (emission spectrometry) and ICP–MS.

For $^{40}Ar/^{39}Ar$ dating, samples were wrapped in Al foil and placed in a cannister. Irradiation lasted 70 hours using fast neutrons at the McMaster reactor. Single-grain $^{40}Ar/^{39}Ar$ stepwise heating analysis was carried out using a LEXEL 3500 continuous 6W argon-ion laser. The proportion of argon isotopes was measured with a MAP 215–50 mass spectrometer equipped with a Nier source and a Johnston MM1 electron multiplier at the University of Montpellier. Measured values of argon were corrected for blanks, atmospheric contamination, mass discrimination, and irradiation-induced mass interference. Radioactive decay of ^{37}Cl and ^{39}Ar were taken into account. Age calculations were done using constants recommended by Steiger & Jäger (1977) and McDougall & Harrison (1988). Errors are 1σ for plateau and total gas ages, and include uncertainties of the ages and $^{40}Ar/^{39}Ar$ values of the standards.